SOME TOPICS IN THE FREE AND FORCED OSCILLATIONS OF A CLASS OF NONLINEAR SYSTEMS

Alexander Vakakis and Thomas Caughey

DYNAMICS LABORATORY REPORT DYNL-89-1

California Institute of Technology

Pasadena, California,

1989

ABSTRACT

In this work we examine the free and forced oscillation of a class of two-Degree-of Freedom Undampted Nonlinear Systems. We examine the existence and stability of Similar Normal Modes of the Unsymmetric system and we analyse the subharmonic periodic orbits of the weakly coupled symmetric oscillator. Furthermore, exact solutions for the steady state forced motions of the strongly nonlinear system, are derived and specific applications for systems with cubic nonlinearities, are given. Finally we give a methodology for examining the Nonsimilar Normal Modes of such systems and we apply the analysis to the case of a weakly coupled system with cubic nonlinearities.

CONTENTS

1. STUDY OF SIMILAR NORMAL MODES

In [1], a methodology was presented for studying the free oscillation of a class of discrete, symmetric, strongly nonlinear systems. These motions were studied by using the concept of "Similar Nonlinear Normal Modes of Free Vibration" introduced first by Rosenberg [2] and it was shown that, depending on the degree of the nonlinearity, more than two normal modes can exist for the system.

In this section, a systematic way for examining the normal modes and their bifurcations, is presented. The "Balancing Diagrams" of Linear and Nonlinear terms are used to study the existence and the bifurcations of similar normal modes in a class of symmetric and unsymmetric systems. Subsequently the stability of these motions is analysed by means of an approximate technique for small values of the amplitudes of oscillation.

1.1. SYMMETRIC SYSTEMS

The system under consideration appears in figure 1 and consists of two lumped masses connected by means of three strongly nonlinear springs. We assume that the two masses are equal to the unit mass , that the two end springs are identical and that the potential function of the system is positive definite and symmetric with respect to the origin of the configuration space. These requirements are satisfied when the stiffnesses of the springs are odd functions of the displacements u:

$$f_1(u) = \sum_{k=1,3,5\ldots} f_{1k}\, u^k = f_3(u) \qquad (1.1)$$

$$f_2(u) = \sum_{k=1,3,5\ldots} f_{2k}\, u^k$$

Throughout this work and unless otherwise stated, the coefficients f_{ij} are assumed to be positive (a same methodology with the one presented here, can be followed when this assumption does not hold).

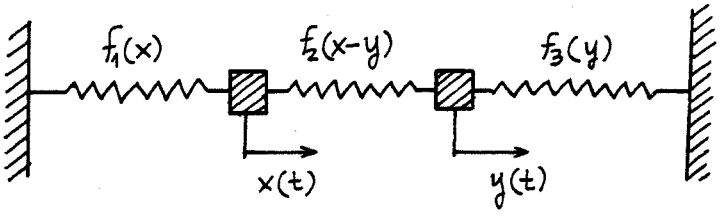

Figure 1. The System under consideration

The equations of motion describing the free oscillations of the system, are:

$$\ddot{x} + \sum_{i=1,3,\ldots} f_{1i}\, x^{i} + \sum_{i=1,3,\ldots} f_{2i}\,(x-y)^{i} = 0$$

$$\ddot{y} - \sum_{i=1,3,\ldots} f_{2i}\,(x-y)^{i} + \sum_{i=1,3,\ldots} f_{1i}\, y^{i} = 0 \qquad (1.2)$$

and the following set of initial conditions is assumed:

$$x(0) = X \qquad y(0) = Y$$

$$\dot{x}(0) = 0 \qquad \dot{y}(0) = 0 \qquad (1.3)$$

Similar normal modes for the system of equations (1.2) can exist, if and only if $y(t)$ and $x(t)$ are related at each instant of time, by a relation of the form:

$$y(t) = c\,x(t) \quad , \quad c \neq 0 \qquad (1.4)$$

where C is a scalar. Substituting (1.4) into (1.2) we get:

$$\ddot{x} + \sum_{i=1,3,\ldots} \left(f_{1i} + f_{2i}\,(1-c)^{i} \right) x^{i} = 0$$

$$\ddot{x} + \sum_{i=1,3,\ldots} \left(f_{1i}\, c^{i-1} - f_{2i}\, \frac{(1-c)^{i}}{c} \right) x^{i} = 0 \qquad (1.5)$$

with initial conditions (1.3) and the addition that $Y = cX$. Both equations (1.5) must be solved with the same set of initial conditions and therefore, for a normal mode to exist it must be satisfied that the coefficients of the respective powers of x in the two equations be equal:

$$f_{1i} + f_{2i}(1-c)^i = f_{1i}\, c^{i-1} - f_{2i}\frac{(1-c)^i}{c} \quad , \quad i = 1, 3, \ldots \qquad (1.6)$$

Hence the question of the existense of similar normal modes for the system of figure 1, is reduced to the study of real roots of c that satisfy all of equations (1.6) simultaneously. By rearranging terms, (1.6) yields:

$$c(1-c^{i-1})\, f_{1i} = (c-1)^i\,(c+1)\, f_{2i} \quad , \quad i = 1, 3, \ldots \qquad (1.7)$$

Certain properties of the real roods for c , were given in [1], namely that $c = \pm 1$, is always a root of (1.7) and that additional real roots are always negative and appear in reciprical pairs (note that we have assumed that $f_{ij} > 0$). The dependence of the quantity c on the ratio of the system parameters , $K_i = f_{2i}/f_{1i}$ is presented in figure 2, for i = 1,3,5 and 7. Each of these diagrams represents the values of c that balance a particular nonlinear term in equations (1.5) and therefore they will be denoted as "Balancing Diagrams". Depending on the number of nonlinear terms in equations (1.5), more than one Balancing Diagrams can exist and it is evident that the value corresponging to a similar normal mode should simultaneously satisfy all the existing Balancing Diagrams of the system.

From the diagrams of figure 2 we see that additional normal modes in the Nonlinear Balancing Diagrams bifurcate from the antisymmetric mode ($c = -1$), the bifurcating value for the ratio being given by:

$$K_{ic} = \left(\frac{f_{2i}}{f_{1i}}\right)_c = \left(\sum_{k=1}^{\frac{i-1}{2}} (-1)^{2k-1}\right) \Big/ 2^{i-1} \quad , \quad i = 3, 5, \ldots \qquad (1.8)$$

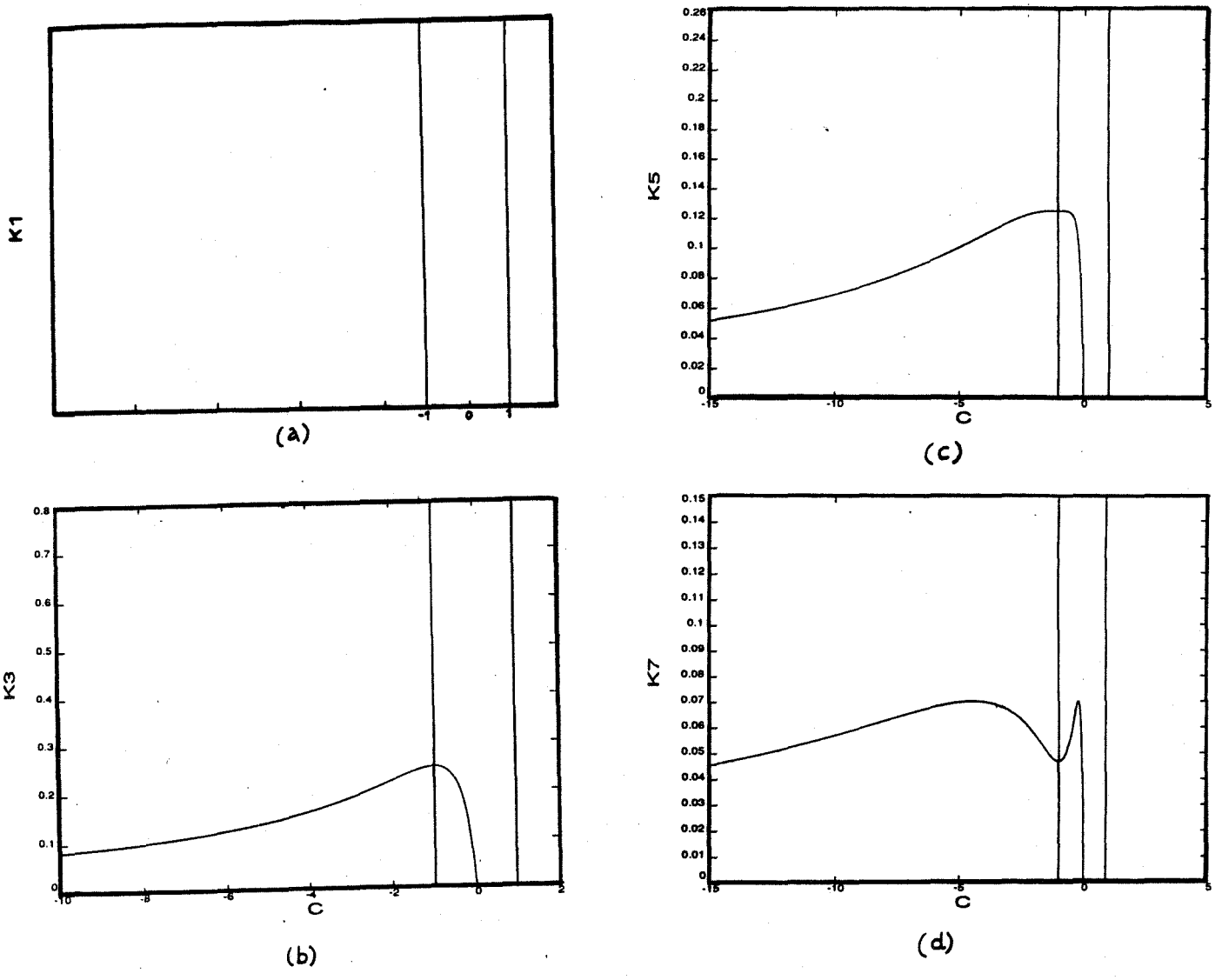

Figure 2: Balancing Diagrams of the symmetric system. (a) Linear, (b) Cubic, (c) Fifth Order (d) Seventh Order

We also conclude, that if the Linear Balancing Diagram exists, i.e. if $f_{21} \neq 0$, the values for C are automatically restricted to $C = \pm 1$, and therefore no additional modes can be realised when the coupling spring has a linear part.

After computing the values of C necessary for similar normal modes, we compute $x(t)$ from any one of equations (1.5) and $y(t)$ from the modal relation (1.4).

1.2. UNSYMMETRIC SYSTEMS

When the symmetry of the systems breaks (unequal end springs or/and masses), the Balancing diagrams of figure 2 are perturbed. To show this, consider the system of figure 1, with stiffneses given by:

$$f_1(u) = \sum_{k=1,3,5,\ldots} f_{1k}\, u^k$$

$$f_2(u) = \sum_{k=1,3,5,\ldots} f_{2k}\, u^k \qquad (1.9)$$

$$f_3(u) = \sum_{k=1,3,5,\ldots} f_{1k}\,(1+\varepsilon_k)\, u^k$$

where ε_k are scalar quantities representing perturbations from the symmetric system. Considering again the equations of motion of the system, imposing the modal relation and matching coefficients in a way similar to the previous section, we obtain the following equations to be satisfied by C :

$$f_{1i} + f_{2i}(1-c)^i = (1+\varepsilon_i)\, f_{1i}\, c^{i-1} - f_{2i}\,\frac{(1-c)^i}{c} \quad , \quad i = 1,3,\ldots \qquad (1.10)$$

The corresponding "perturbed" Balancing Diagrams appear in figure 3, for $\varepsilon_1=\varepsilon_3=\varepsilon_5=\varepsilon_7=0.05$. Note that we have nowhere made the assumption of ε_i being small and therefore, the methodology presented here is also valid for unsymmetric systems with large structural perturbations ε_i .

A first general conclusion, concering the free oscillations of the unsymmetric system, is that due to the lack of symmetry, the symmetric and antisymmetric modes cannot be materialised in this case and that the bifurcating modes do not appear any more in reciprical pairs. Again the necessary value of C for similar normal modes, should satisfy all the Balancing Diagrams of the system and therefore an examination of the free oscillations of unsymmetric systems must be carried out on a case to case basis.

1.3. APPLICATIONS - STABILITY CONSIDERATIONS

Application of the method to symmetric systems, were given in [1] and therefore here we will be only concerned with unsymmetric ones. Two unsymmetric systems will be examined. In the first case, only one Balancing Diagram needs to be satisfied, whereas in the second case, in addition to a Nonlinear Balancing diagram, a Linear one also exists. In each case, the similar normal modes are computed and a stability analysis is subsequently carried out.

1.3.1. UNSYMMETRIC SYSTEM WITH ONE BALANCING DIAGRAM

Consider a system with stiffnesses given by:

$$\begin{aligned} f_1(u) &= u+u^7 \\ f_2(u) &= K_7 u^7 \\ f_3(u) &= u+\varepsilon u^7 \end{aligned} \qquad (1.11)$$

In the terminology of the theory outlined in previous sections, this is an unsymmetric system with structural pertubations $\varepsilon_1=0$, $\varepsilon_7=1-\varepsilon$ and $\varepsilon_i=0$, $i=3,5,9,\ldots$.

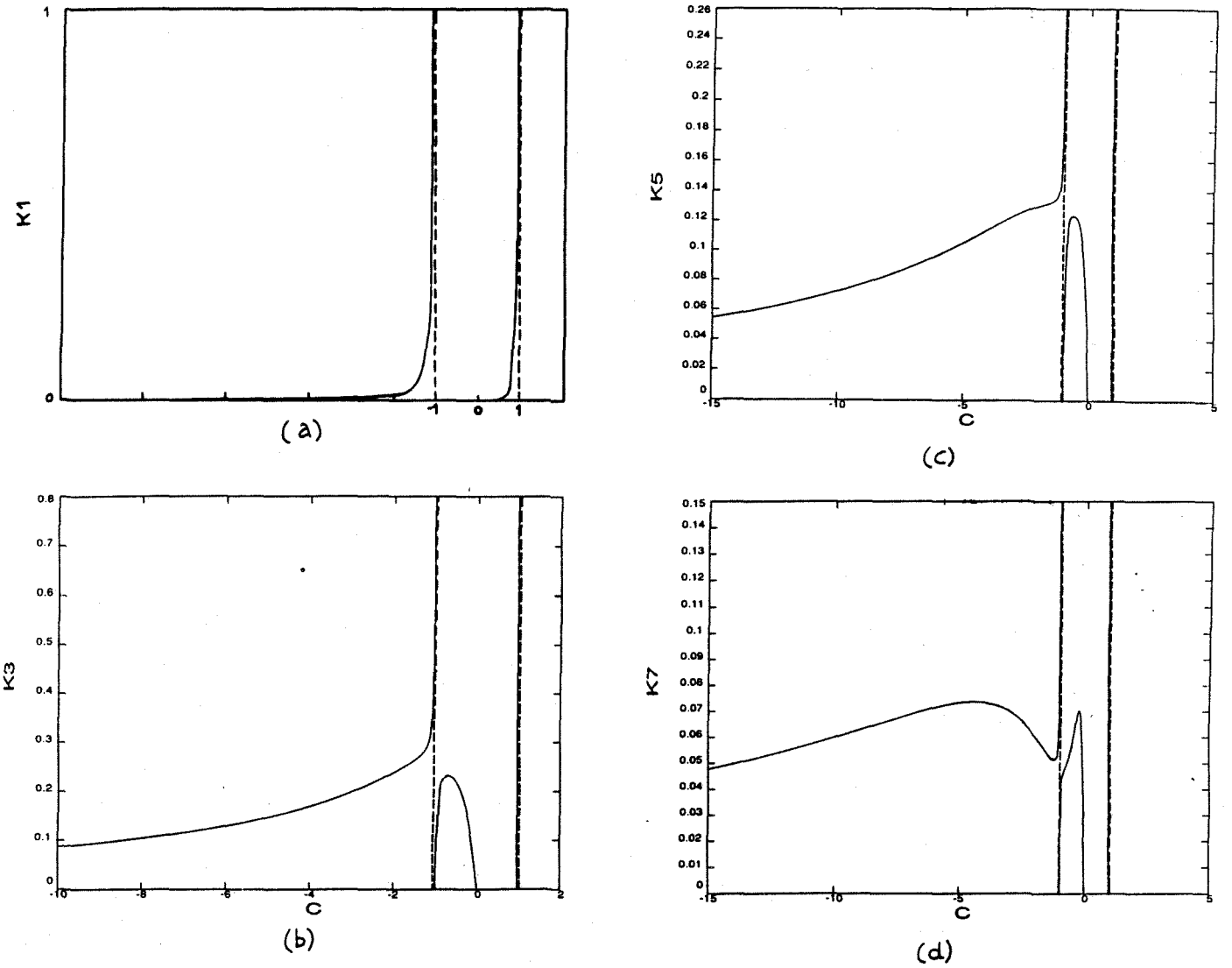

Figure 3. Balancing Diagrams of the Unsymmetric system.
(a) Linear, (b) Cubic, (c) Fifth order
(d) Seventh Order.

The differential equations of motion take the form:

$$\ddot{x}+x+x^7+K_7(x-y)^7=0$$
$$\ddot{y}+y+\varepsilon y^7+K_7(y-x)^7=0 \qquad (1.12)$$

and have to be solved with initial conditions (1.3). By setting $y=cx$ and $Y=cX$, equations (1.12) transform to :

$$\ddot{x}+x+x^7+K_7(1-c)^7x^7=0$$
$$\ddot{x}+x+\varepsilon c^6x^7+K_7\frac{(c-1)^7}{c}x^7=0 \qquad (1.13)$$

and $x(0)=X$, $\dot{x}(0)=0$.

We see that the linear terms in (1.13) are balanced for every value of c and therefore we only need examine the seventh order Balancing Diagram for this system, given by:

$$1+K_7(1-c)^7=\varepsilon c^6+K_7\frac{(c-1)^7}{c} \qquad (1.14)$$

Note that we could have obtained the above equation directly from expresion (1.10) by setting $i=7$, $f_{27}/f_{17}=K_7$ and $1+\varepsilon_7=\varepsilon$. For a fixed value of ε, equation (1.14) gives the Balancing Diagram of figure 3(d) and we see that the system posseses two, four or six real roots for c, depending on the numerical value of the parameter K_7. Using these values of c, we can uncouple the equations of motion and each of equations (1.13), will give the same result for the response $x(t)$, the actual waveforms being computed by means of the formulas devived in [1] for the free oscillation of a one Degree-of-Freedom system. Subsequently we compute the waveform for $y(t)$, with the modal relation $y(t)=cx(t)$.

As far as the stability of these motions is concerned, it was pointed out in [2], that the normal modes are never Liapunov stable and therefore at most we can expect orbital stability to occur. In order to investigate the free vibrations of the system under consideration, we use the methodology of reference [3].

The basic steps of the stability analysis can be found in [1,3] and will not be repeated here. We only state that the variational equations of the system are of Hill-type and are reduced to "equivalent" Mathiew equations by omitting certain higher harmonic terms.

For the system under consideration, the resulting set of Mathiew equations is of the form (for details of the stability analysis, see [1]):

$$\ddot{\xi}+\xi\left(1+\frac{7}{21}A_5\,v^{*6}\right)=0$$

$$\ddot{\eta}+\eta\left(1+7A_2\,v^{*6}\right)=0 \qquad (1.15)$$

where: $v^*(t)=\beta\cos\left(1+A_2\frac{35\beta^6}{128}\right)t+O(\beta^2)$, $\ddot{(\,)}\equiv d^2/dt^2$

$$A_5=\frac{21}{(1+c^2)^4}\left[K_7(1+c)^2(1-c)^6+c^2(1+\varepsilon c^4)\right]$$

$$A_2=\frac{1}{(1+c^2)^4}\left[K_7(1-c)^8+1+\varepsilon c^8\right]$$

In (1.15), β represents the amplitude of oscillation of the v-coordinate and $\xi(t)$, $\eta(t)$ represent small perturbations from the normal mode in the directions u and v respectively (see figure 4).

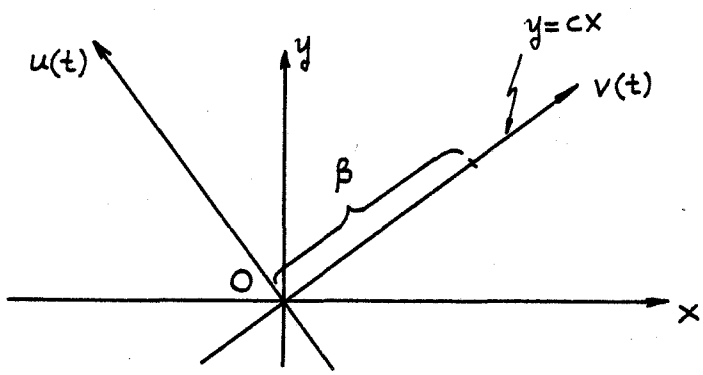

Figure 4. Coordinate system for stability analysis

The motion corresponding to the η -variational equation has two characteristic exporents equal to zero and therefore, the

stability of the mode under consideration, is determined only from the ξ-variational equation. By changing the independent variable t to τ, we obtain:

$$\xi'' + (\delta_1 + 2\theta_1 \cos 2\tau)\xi = 0$$
$$\tau = \left(1 + A_2 \frac{35\beta^6}{128}\right) t \quad , \quad ( )'' \equiv d^2/d\tau^2$$
$$\delta_1 = 1 - \frac{35}{64} A_2 \beta^6 + \frac{35}{336} A_5 \beta^6 \qquad (1.16)$$
$$\theta_1 = \frac{105}{1344} A_5 \beta^6$$

We note that the above stability analysis is only approximate and is valid for small values of the amplitude β [1,3].

In figure 5, we present the stability characteristics of (1.16) in the Stutt Diagram, for various values of the structural parameter K_7. In order to compute a point of these graphs, we assigned a value to K_7 and computed the corresponding values of c, from (1.14) and of δ_1, θ_1, from (1.16). The perturbation parameter ϵ was taken $\epsilon = 1.05$ and $\beta = 0.9$.

The stability results for the free oscillations of the system are presented in Figure 5. Before discussing the results, we must remark that for the corresponding symmetric system ($\epsilon=1.0$), it was found that two Saddle Node and one Pitchfork, bifurcations occur in the Balancing Diagram (figure 17[1]). We now observe that the unsymmetry has resulted in a destruction of the Pitchfork Bifurcation and in its place a Saddle Node Bifurcation appears (denoted by ③). This had to be expected, since the pitchfork Bifurcation is a result of a rotational symmetry of a strucutre and is structurally unstable. On the contrary, Saddle Node Bifurcations are generic for this class of systems [4].

From figure 5(b), we see that the unsymmetric system can have two, three or four stable free oscillations depending on the value of the structural parameter K_7. Furthermore, it can be shown that the stability analysis shown here is independent of the aplitude β and (as will become evident latter) this is a result of the fact that only one Balancing Diagram is needed for

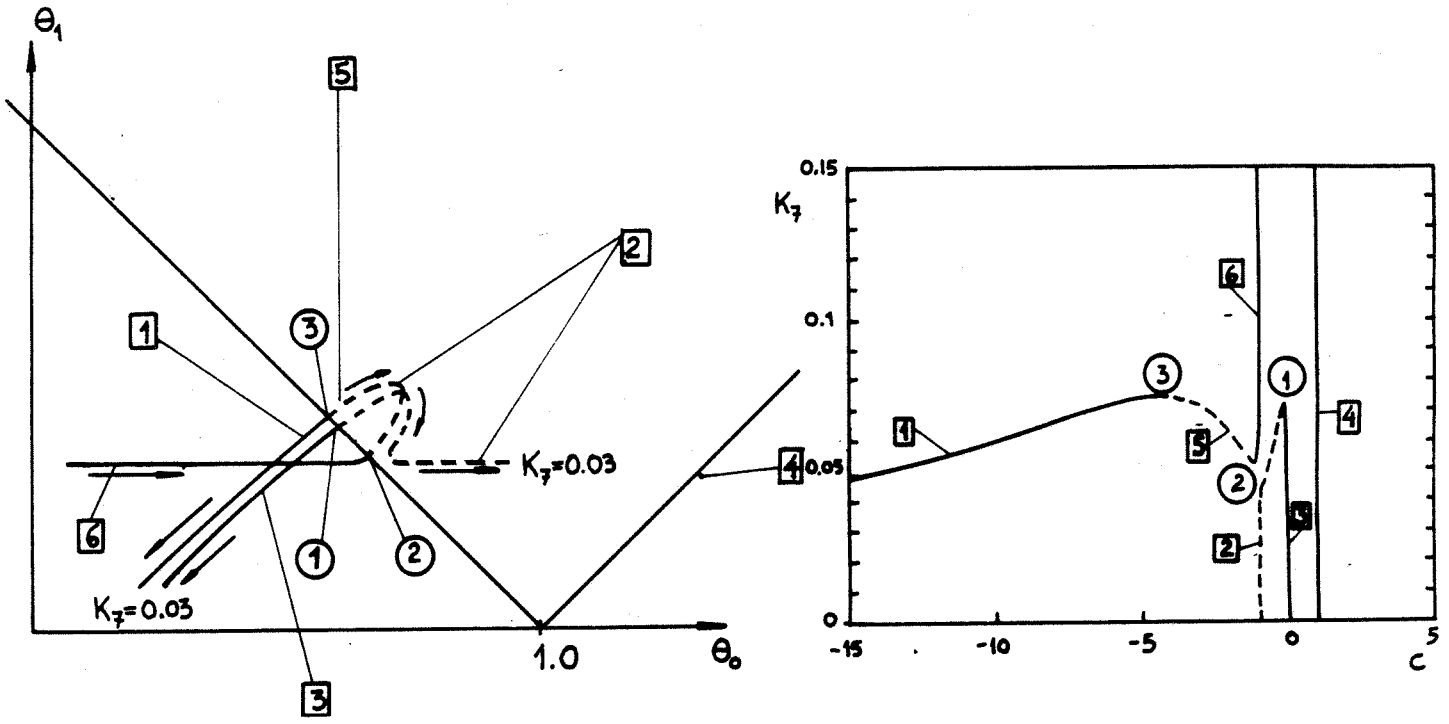

Figure 5. Stability Analysis for the Unsymmetric system of section 1.3.1. (a) Arrows in the direction of decreasing K_7. (b) Solutions stable _____, unstable-----.

the study of free oscillations of this system. Note that although the stability analysis presented here is only approximate (and thus is valid only for low amplitudes), the stability results can be extended to large amplitudes β by means of Poincaré map techniques as will be shown in the next sections.

Concluding the stability analysis, we state that three Saddle Node bifurcations exist in the Balancing Diagram of this system and the stability results do not depend on the amplitude β or on the structural perturbation $\varepsilon_7=1-\varepsilon$. As we will demonstrate shortly, these results do not hold when a system posses more than one Balancing Diagrams.

1.3.2. UNSYMMETRIC SYSTEM WITH TWO BALANCING DIAGRAMS

We will now demonstrate the effect of introducing an additional Balancing Diagram in the unsymmetric system with seventh order nonlinearity of section 1.3.1. Assume to this end that the stiffnesses of the system are given by:

$$f_1(u) = u + u^7$$

$$f_2(u) = K_1 u + K_7 u^7 \qquad (1.17)$$

$$f_3(u) = \varepsilon(u + u^7) = \varepsilon f_1(u)$$

Note that we have introduced a linear term in the expression for the coupling spring and that we have also perturbed the linear part of the right end spring. Using the modal relation $y = cx$, the equations of motion take the form:

$$\ddot{x} + x\left[1 + K_1(1-c)\right] + x^7\left[1 + K_7(1-c)^7\right] = 0$$

$$\ddot{x} + x\left[\varepsilon + K_1\frac{(c-1)}{c}\right] + x^7\left[\varepsilon c^6 + K_7\frac{(c-1)^7}{c}\right] = 0 \qquad (1.18)$$

and we immediately see that we have to match linear and seventh order terms. We therefore conclude that two Balancing diagrams are required for the analysis of the free oscillations of this system:

$$c(\varepsilon - 1) = K_1(1 - c^2) \quad \text{(Linear Bal. Diag.)} \qquad (1.19)$$

$$c(\varepsilon c^6 - 1) = K_7(1 - c^2)(1 - c)^6 \quad \text{(Seventh Order Bal. Diag.)}$$

A necessary condition for similar normal modes, is that c satisfies both equations (1.19), or equivalently both of the Diagrams 3(a) and 3(d). The stability analysis for these free oscillatory motions is performed in exactly the same manner as

before and the ξ - variational equation for this system (equivalent to (1.16) of previous section), is given by:

$$\xi'' + (\delta_1 + 2\theta_1 \cos 2\tau + \zeta_1 \cos 4\tau + s_1 \cos 6\tau)\xi = 0$$

$$\delta_1 = \frac{A_{11}}{A_0} - \frac{35}{64}\frac{A_2 A_{11}}{A_0^2}\beta^6 + \frac{35}{336}\frac{A_5}{A_0}\beta^6$$

$$\theta_1 = \frac{105}{1344}\frac{A_5}{A_0}\beta^6$$

$$\zeta_1 = \frac{21}{336}\frac{A_5}{A_0}\beta^6$$

$$s_1 = \frac{7}{672}\frac{A_5}{A_0}\beta^6$$

where $( )'' \equiv d^2/d\tau^2$, $\tau = \left(A_0^{1/2} + \frac{A_2}{A_0^{1/2}}\frac{35\beta^6}{128}\right)t$

$$A_{11} = \frac{1}{(1+c^2)}\left[c^2 + \varepsilon + \frac{(\varepsilon-1)c(1+c)}{1-c}\right]$$

$$A_0 = \frac{c}{(1+c^2)}\left[\left(\frac{\varepsilon-1}{1-c^2}\right)(1-c)^2 + \frac{\varepsilon c^2+1}{c}\right]$$

A_5, A_2 are given by (1.15) and β and $\xi(\tau)$ are defined in the previous section. To calculate the above expressions, we have expressed K_1 as a function of c from the first of equations (1.19). The computation procedure can then be summarised as follows: For each value of K_7, compute the roots of c from the second of equations (1.19). Then use this value of c to compute the necessary value of K_1 for the system. Finally use the obtained values of c, K_1 and the assigned value for K_7 to compute the coefficients δ_1 and θ_1 of the Mathiew equation.

It turns out that ζ_1 and s_1 are small when β is small and therefore the stability characteristics of these terms when K_7 varies are outside the secondary instability regions (for a discussion of the approximate stability of Hill's equation, see

Hayashi [5]). So our main concern is the primary instability region as in the previous section.

Two different applications are given. In the first, we took $\varepsilon=1.05$, $\beta=0.9$ and the stability characteristics are presented in figure 6. For the second application we had $\varepsilon=1.2$, $\beta=0.9$ and the stability characteristics for this system are plotted in figure 7. We observe that by varying the parameter ϵ (giving the meassure of the unsymmetry of the system), the stability of the free vibration of the system is altered. It can be also shown that the stability of the modes of the system, depends on the amplitude of motion, in contrast to the system of the previous section. Finally, no such thing as Saddle-Node Bifurcations, can be detected in the Balancing Diagrams of this unsymmetric system.

From figures 6,7 we note that if c takes values in the range $c\in(-1,0)$, it is necessary that $K_1<0$. When K_1 and K_7 are restricted to be positive, then c must only be in the range $c\in(-\infty,-1)\cup(0,1)$. The symmetric mode [4] is not shown in the above figures, but it is well inside the stable region and therefore is orbitally stable.

So we conclude that when more than one Balancing Diagrams are involved, the stability of a mode depends on the amplitude and the degree of asymmetry of the system. To the contrary, when only one Balancing Diagram exists, the stability results hold independently of the amplitude of motion or the degree of unsymmetry of the system and Saddle - Node Bifurcations of modes replace the Pitchfork bifurcations observed in the symmetric system.

We end this section by mentioning that Rosenberg [2] predicted the independence of stability from the amplitude for "Homogeneous" systems, i.e. for systems with stiffness proportional to the same power of the displacement. In this work, we observed the same result for systems that were not homogeneous (the end springs contained also a linear term), but which they possesed only one Balancing Diagram of Nonlinear terms. Thus, the criterion for the independence of the mode stability from the amplitude, appears to be the existense of only one Balancing Diagram for the system.

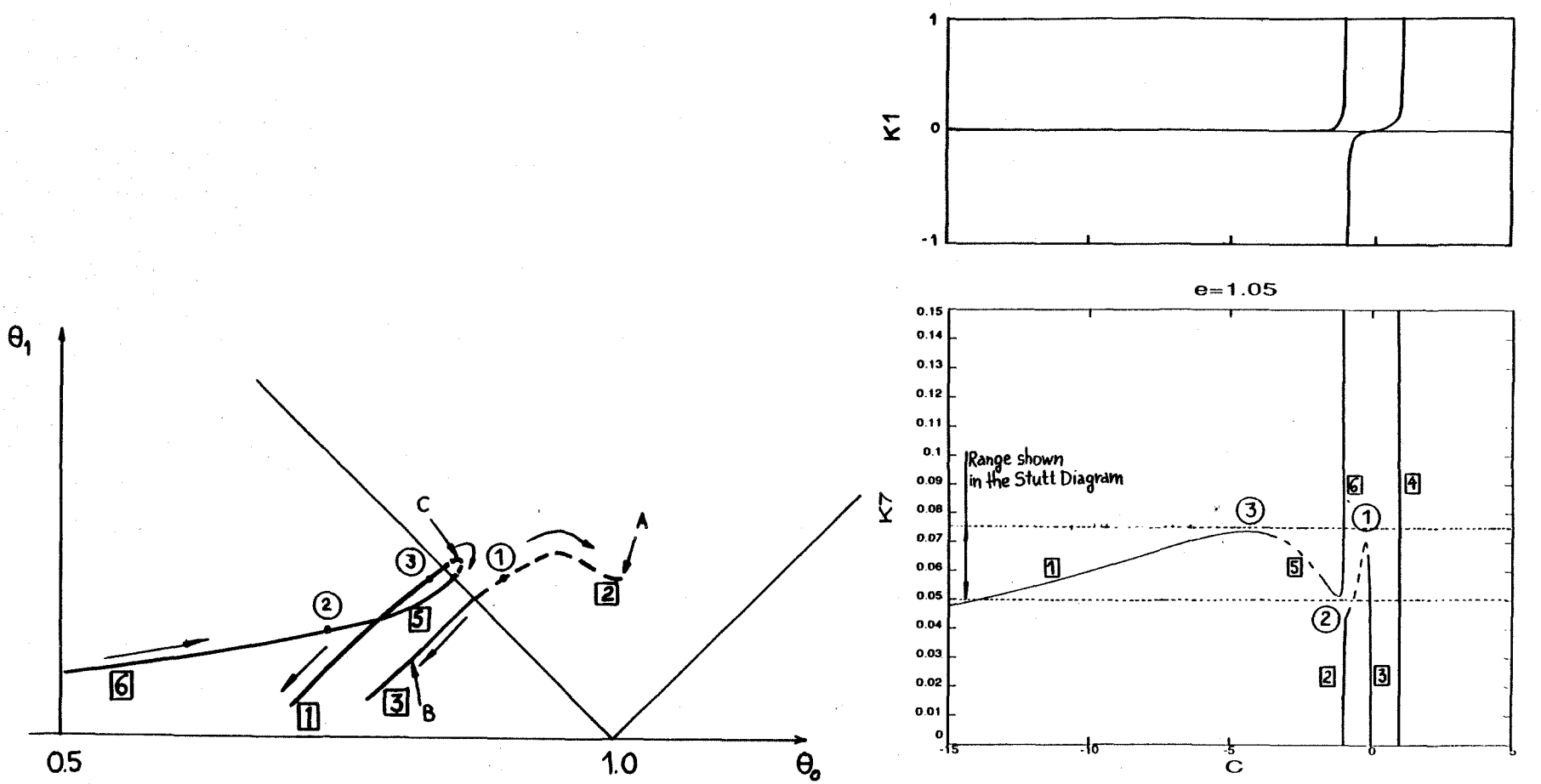

Figure 6: Stability analysis of the Unsymmetric System of section 1.3.2, $\varepsilon = 1.05$, $\beta = 0.9$. (a) Arrows in the direction of decreasing K_7 (b) Solutions stable _____, ustable --------.

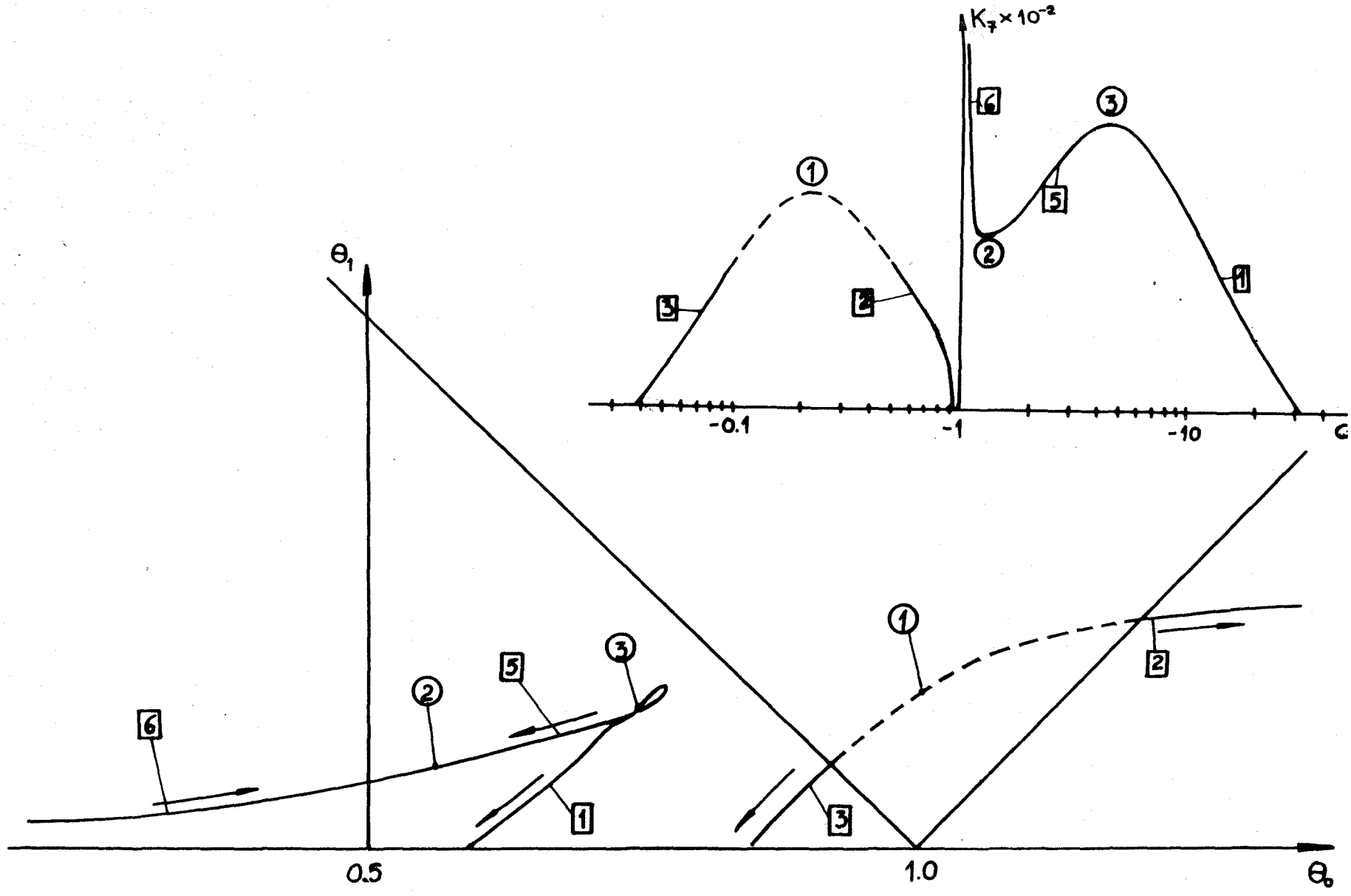

Figure 7: Stability analysis of the Unsymmetric system of section 1.3.2, $\varepsilon = 1.20$, $\beta = 0.9$.
(a) Arrows in the direction of decreasing K_7
(b) Solution stable _____ unstable - - - - - -

1.4. SPECIAL PERTURBATIONS OF THE SYMMETRIC SYSTEM

In the previous sections we have found that a perturbed asymmetric system cannot possess the $c = \pm 1$ modes of free oscillation. In this section we will demonstrate how by introducing special "symmetric" perturbations in the systems, the symmetric and asymmetric modes can be retained. We will demonstrate this by means of an example.

Consider the system with cubic nonlinearities described by the following differential equations of motion:

$$\ddot{x} + f_{13}\, x^3 + f_{23}\,(x-y)^3 = 0$$

$$\ddot{y} + f_{13}\, y^3 - f_{23}\,(x-y)^3 = 0$$

In [1] it was shown that the above symmetric system posseses the following Balancing Diagram of cubic terms ($K_3 = f_{23} / f_{13}$).

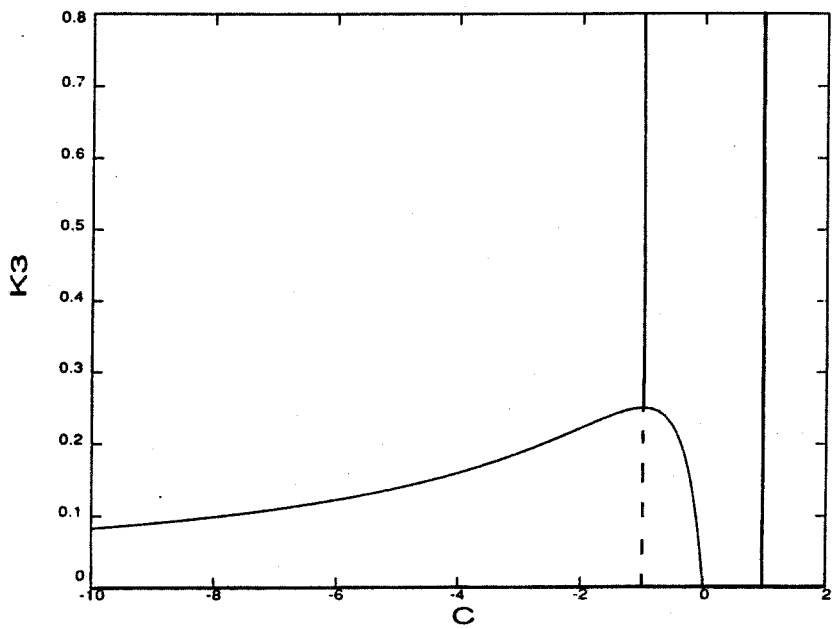

Figure 8: Symmetric System with cubic Nonlinearities.
Solutions Stable _____ Unstable -------.

We now perturb the above set of equations as follows:

$$\ddot{x} + f_{13}\, x^3 + \left[f_{23}\,(x-y)^3 + \varepsilon\,(x+y)^2 x \right] = 0$$

$$\ddot{y} + f_{13}\, y^3 - \left[f_{23}\,(x-y)^3 + \varepsilon\,(x+y)^2 y \right] = 0 \qquad (1.21)$$

The perturbation terms in the differential equations of motion (1.21) cannot be realised by passive elements (stiffnesses etc), but they rather represent feedback applied on the system (1.21). Note also the symmetry of the perturbed system. Seeking normal modes , we follow the matching procedure outlined previously, which leads to the following equation for c :

$$K_3 = \frac{f_{23}}{f_{13}} = -\frac{c}{(1-c)^2} + \frac{\varepsilon}{f_{13}} \frac{(1+c)\,c}{(1-c)^2} \qquad (1.22)$$

Equation (1.22) represents a perturbation of the Balancing Diagram of the symmetric system and it is plotted in Figure 9. We see that the perturbed system possesses the $c = \pm 1$ symmetric and antisymmetric normal modes. Note that the Pitchfork Bifurcation of figure 8, is replaced by a Transcritical and a Saddle Node bifurcation. When we introduce an asymmetry in equations (1.21) we expect the structurally unstable Transcritical Bifurcation to break up.

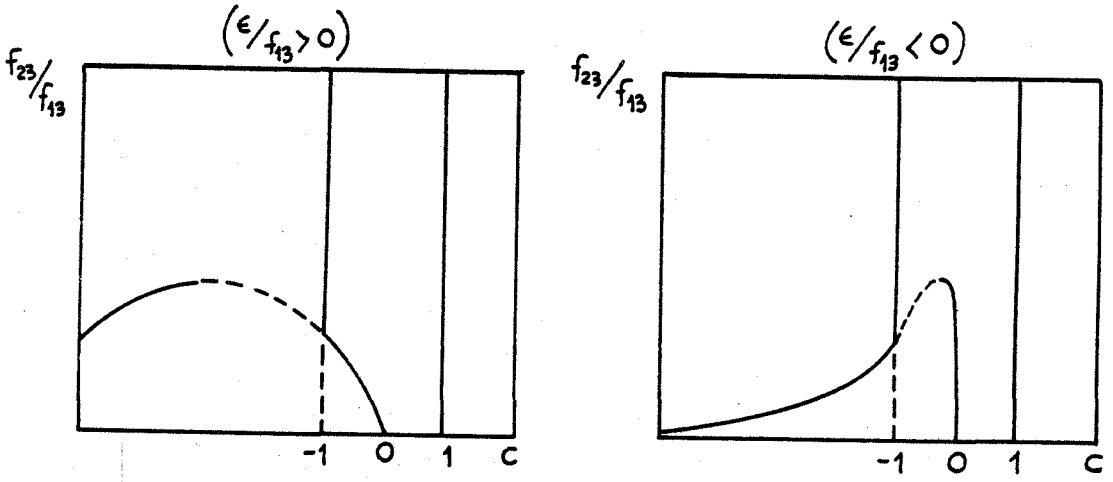

Figure 9: Perturbed Balancing Diagrams.
Solutions Stable_____ Ustable-------.

2. USE OF THE POINCARE MAP FOR THE DETERMINATION OF THE STABILITY OF NORMAL MODES

The idea of using the Poincare Map to study the stability of the similar normal modes of a system, was first reported in [6,7]. The use of the Poincare Map has certain advantages over the approximate method outlined in the previous section, since it gives us a global picture of the flow field of the dynamical system in the neighborhood of a normal mode and therefore it leads to a better stability picture than that obtained by the approximate stability technique. Certain deficiencies of the approximate technique are resolved, such as the question of the mode stability for large amplitudes and the stability indeterminancy of the symmetric mode for the symmetric system.

2.1. POINCARE MAP FOR A TWO DEGREE OF FREEDOM SYSTEM

Consider the two DOF system of figure 1. It is a Hamiltonian system with a four dimensional phase space $(x, \dot{x}, y, \dot{y})$. Consider the flow of this dynamical system in the phase space and restrict it to be on a constant energy (Hamiltonian) level. We achieve this by imposing the condition

$$H(x, \dot{x}, y, \dot{y}) = h \qquad (2.1)$$

where $H(\cdot)$ is the expression of the Hamiltonian of the system and h is the particular level of energy. Then instead of considering the full four dimensional phase space we examine the flow on the three dimensional hypersurface given by expression (2.1). The Hamiltonian H is a first integral of motion for the system and in this case represents conservation of energy during a free oscillation. If another first integral of motion, independent from the Hamiltonian, exists, then the two DOF system is "integrable" and the energy manifold $H = h$ is fibered by invariant two-dimenstional tori [6,7]. It must be pointed out that integrability is not generic in Hamiltonian systems and thus generally we do not expect a second independent integral of motion to exist.

Now suppose that we intersect the three dimensional energy manifold defined by (2.1), by another two dimensional plane. If the intersection is transverse [4], the resulting cross section Σ is two dimensional, and the flow intersecting the plane defines an orientation preserving map, the so called Poincaré Map (in figure 10, under the flow, point A is mapped to point A').

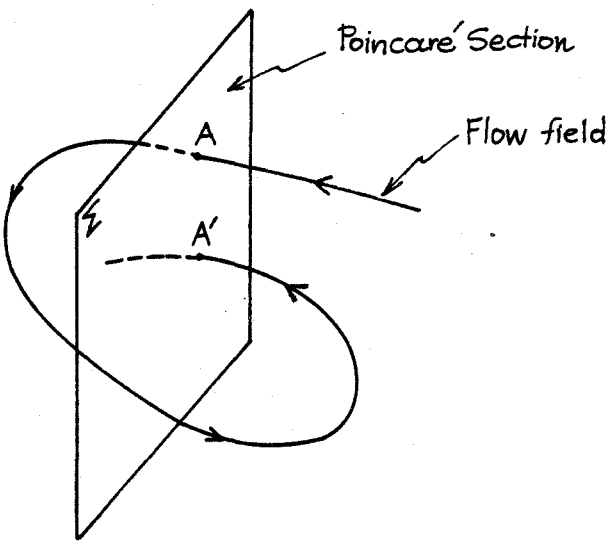

Figure 10. Poincaré Map

A convenient two dimensional plane for slicing the energy manifold is the plane T [6,7]:

$$T: \; x = 0 \tag{2.2}$$

and therefore the plane Σ of figure 10, is defined as $\Sigma = \{x=0\} \cap \{H=h\}$. In order for Σ to exist, the intersection must be transverse and for this we require that the normal to the slicing surface $\{x=0\}$ be not perpendicular to the tangent of the flow field $(x, \dot{x}, y, \dot{y})$. This means that

$$(\dot{x}, \ddot{x}, \dot{y}, \ddot{y}) \cdot (1,0,0,0) \neq 0 \Rightarrow \dot{x} \neq 0 \tag{2.3}$$

(Transversality Condition)

and we impose the additional condition that $\dot{x} > 0$, in order that the flow field pierce the section Σ always from the "same side" (and the Poincaré Map be orientation preserving).

As shown in [6,7], a Poincaré Map can be formed analytically as long as a second independent integral of motion exists, but unfortunatelly this is not the generic case. In non-integrable cases, approximate first integrals can be still formed for low energies h and for a discussion of the various techniques see [6].

A free oscillation of the system corresponding to a similar normal mode, will be a periodic motion and therefore it will pierce the Poincaré Section Σ only once. Hence a similar normal mode will appear in the Poincaré Map as a fixed point and its stability can be determined by observing the nature of the Poincaré Map of nearby motions (i.e. of motions that result as small perturbations of the mode). If a mode is orbitally stable, then the corresponding fixed point of the Poincaré Map must be stable too and it should be surrounded by concentric closed curves, appearing as a center. On the contrary, an unstable normal mode should appear in the Poincaré Map as a saddle point.

Before considering applications of the Poincaré Map, we should note that the above stability analysis is only valid for small energies h. This is because, generally the two DOF nonlinear oscillator will not possess a second independent integral of motion and hence the system will not be integrable. For such nonintegrable 2 DOF systems, we know from KAM (Kolmogorov - Arnold- Moser) theory, that "rational" tori break, resulting in layers of ergodic motion, filling the phase space between sufficiently "irrational", preserved tori [8]. As the energy level h increases, we typically expect all the tori to break, resulting in the filling of the whole phase space with ergodic motion.

2.2. APPLICATION TO A SYMMETRIC SYSTEM

We will apply the technique outlined in the previous section, for the case of the two Degree of Freedom Symmetric Oscillator of figure 1, with stiffnesses given by:

$$f_1(u) = u + u^3$$

$$f_2(u) = K_3 u^3$$

$$f_3(u) = u + u^3 \qquad (2.4)$$

The same system was analysed in [6] and we only do the analysis, to demonstrate the effect that the increase of energy has on the Poincaré Map of this system.

The Hamiltonian of this system is given by:

$$H(x,\dot{x},y,\dot{y}) = \frac{1}{2}(x^2+y^2) + \frac{1}{4}(x^4+y^4+K_3(x-y)^4) + \frac{1}{2}((\dot{x})^2+(\dot{y})^2) \qquad (2.5)$$

where $\dot{x}$ and $\dot{y}$ are equal in this case to the generalised momenta. We consider the energy manifold for level $H=h$ and we generate the Poincaré Map by setting $x=0$. This results in the following expression for $\dot{x}$:

$$\dot{x} = \left[2h - \frac{1}{2}(1+K_3)y^4 - y^2 - (\dot{y})^2 \right]^{1/2} \qquad (2.6)$$

By construction, the Poincaré section will contain the points $(y, \dot{y})$ corresponding to $x=0$ and $\dot{x}>0$. Thus the Poincaré Map will fill the interior of a region with boundary

$$2h = \tfrac{1}{2}(1+K_3)y^4 + y^2 + (\dot{y})^2 \qquad (2.7)$$

corresponding to $\dot{x}=0$.

The plan is to integrate numerically the differential equations of motion of the system and plot the values of $(y, \dot{y})$ corresponding to $x=0$ and $\dot{x}>0$. These graphs will give us the Poihcaré Maps of the system. Here we recall that the Balancing Diagram for this nonlinear Oscillator is given by figure 11 and we see that there exist either two or four similar normal modes of free oscillation, in the later case one of them being unstable.

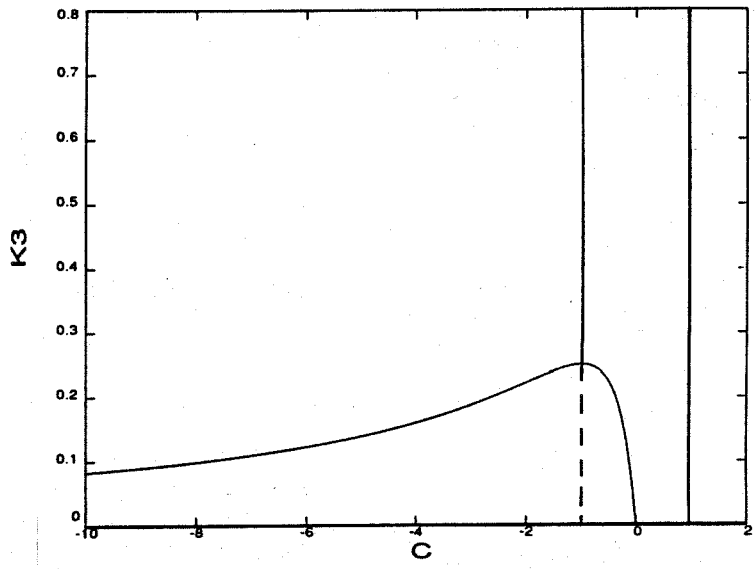

Figure 11: Cubic Balancing Diagram
Modes Stable _____ Unstable ------

In figure 12*, we present the numerically computed Poincaré Map for the system with $K_3 = 0.4 > 1/4$. We see that the two existing similar normal modes are orbitally stable, since they appear as centers in the Poincaré Maps.

In figure 13, we present the Poincaré Maps for the system with $K_3 = 0.1 < 1/4$, i.e. a system with four similar normal modes. For low energies (figure 13(a)), the unstable normal mode appears as a saddle point, whereas the other three modes are orbitally stable. As we increase the energy level, we observe a "sea of stochasticity" [8] filling gradually the Poincaré Map and this is an indication of the nonintegrability of the system. Another point to be observed is the existense of subharmonic orbits consisting of elliptic periodic points (surrounded by "islands" of closed curves) and hyperbolic points (unstable saddles). These elliptic-hyperbolic points are the result of the breakdown of resonant invariant KAM tori, and they will be investigated in the next section.

3. STUDY OF SUBHARMONIC ORBITS IN THE SYMMETRIC SYSTEM

In this section we will use the perturbation methods developed by Holmes and Marsden [9,10], to prove the existense of arbitrarly many periodic orbits in the neighborhood of an orbit of the two degree of freedom symmetric Hamiltonian system with cubic nonlinearities. In [11,12] this methodology was applied to prove the nonexistense of analytic second integrals of motion of a certain type and to study the way in which resonant tovi break up between KAM "irrational" preserved tori, for a pair of weakly coupled penduli. We will follow the methodology of these references and we will prove the existense of the subharmonic periodic orbits, that were observed in the numerical Poincaré plots of figure 13.

3.1. ANALYSIS, VEERMAN - HOLMES THEOREM

Throughout this analysis we will consider the symmetric Hamiltonian system of figure 14. This system consists of two coupled single DOF nonlinear oscillators and when the coupling is

---

* We would like to appreciate the help of J. Sivo, for developing the computer programs for these Poincaré Plots.

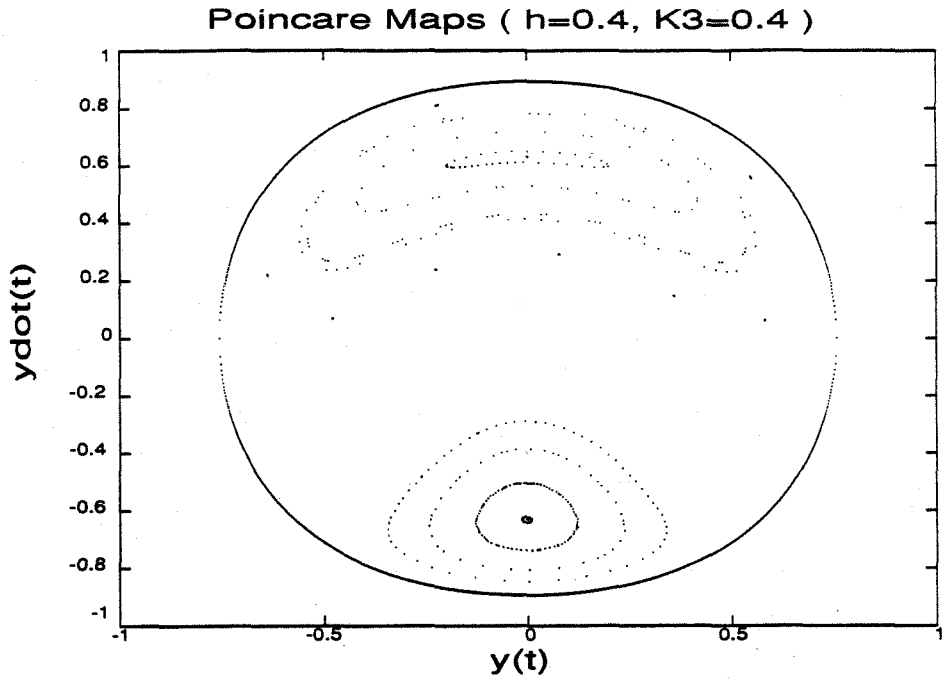
Poincare Maps (h=0.4, K3=0.4)
ydot(t)
y(t)
1
0.8
0.6
0.4
0.2
0
-0.2
-0.4
-0.6
-0.8
-1
-0.5
0.5

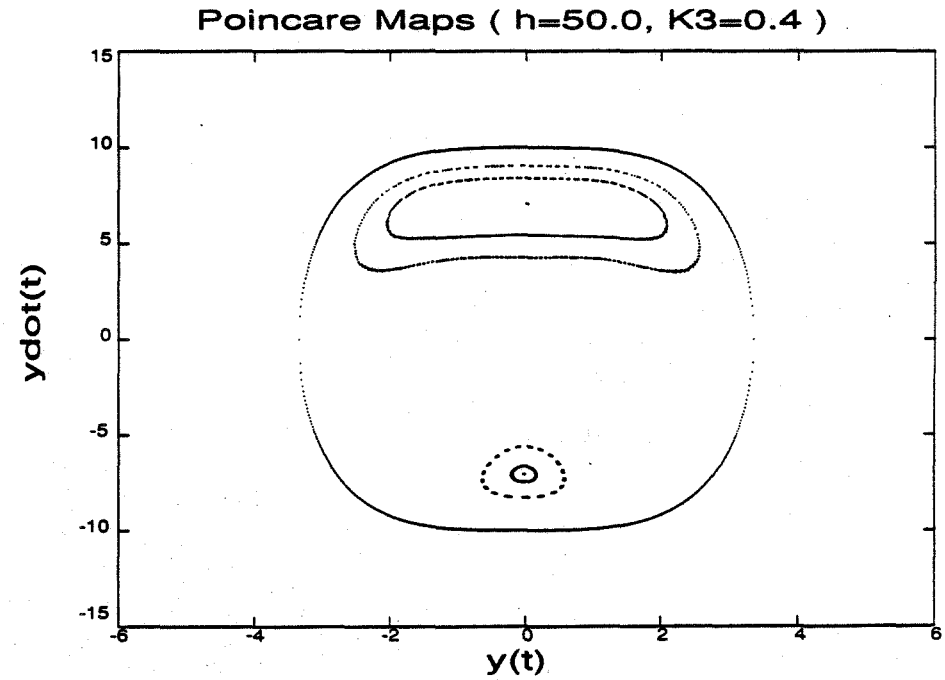
Poincare Maps (h=50.0, K3=0.4)
ydot(t)
y(t)
15
10
5
0
-5
-10
-15
-6
-4
-2
2
4
6

Figure 12

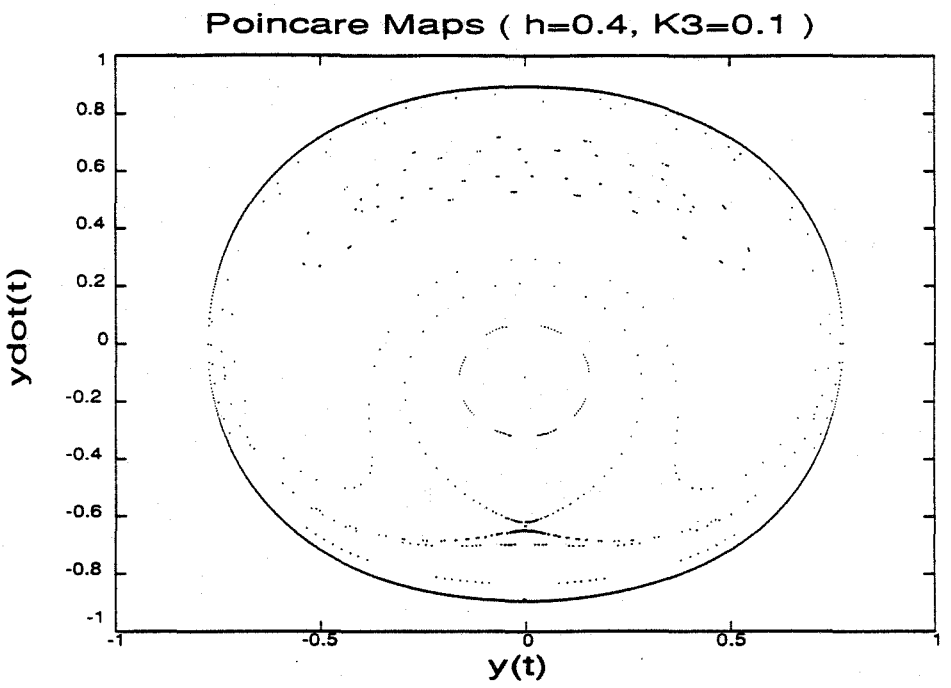
Poincare Maps (h=0.4, K3=0.1)
ydot(t)
y(t)
1
0.8
0.6
0.4
0.2
0
-0.2
-0.4
-0.6
-0.8
-1
-0.5
0.5

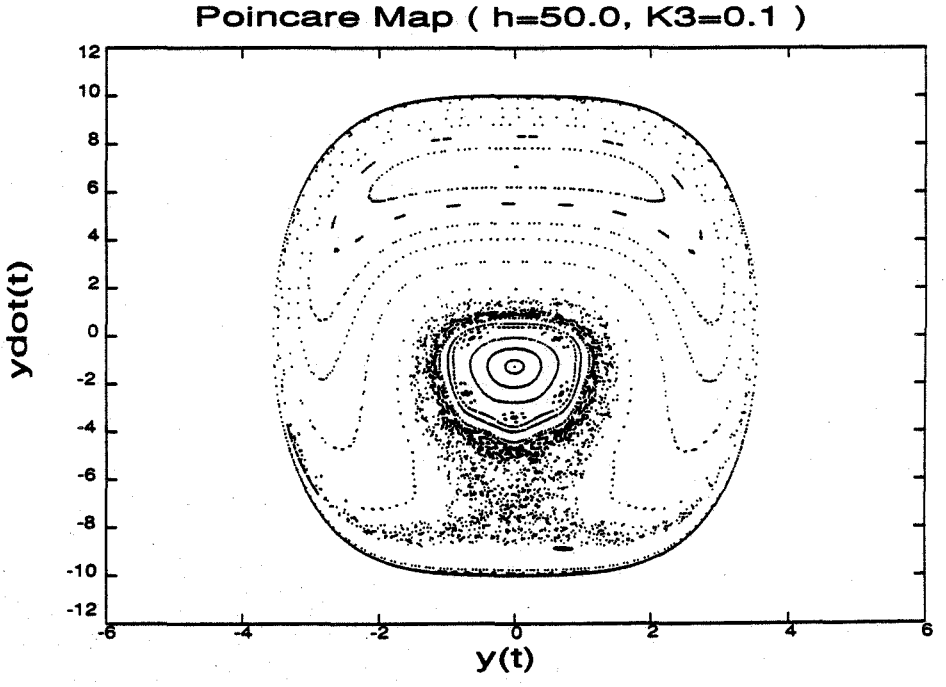
Poincare Map (h=50.0, K3=0.1)
ydot(t)
y(t)
12
10
8
6
4
2
0
-2
-4
-6
-8
-10
-12
-6
-4
-2
2
4
6

Figure 13

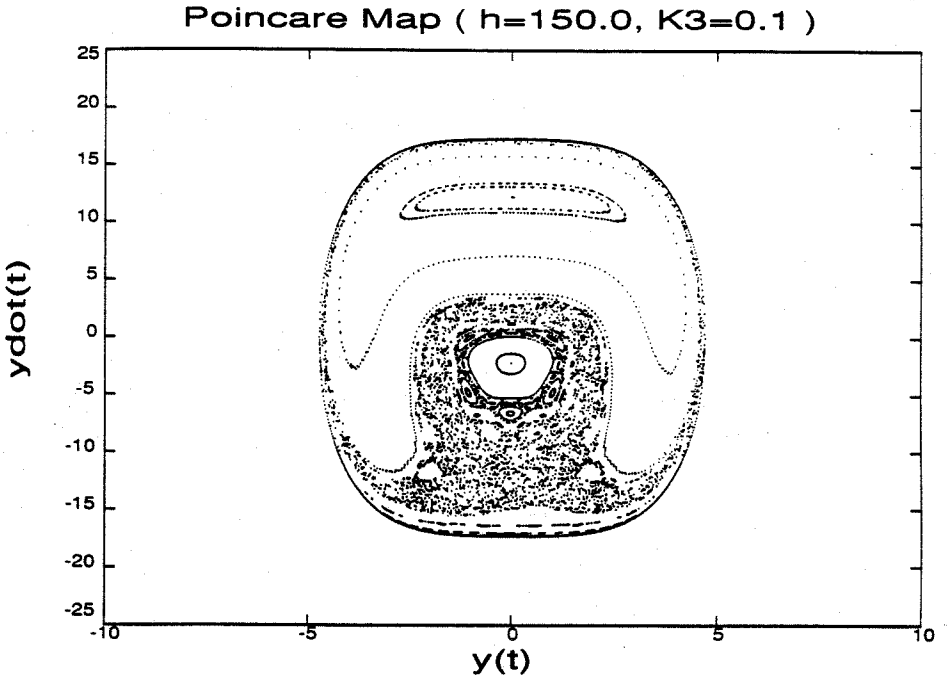
Poincare Map (h=150.0, K3=0.1)
ydot(t)
y(t)
25
20
15
10
5
0
-5
-10
-15
-20
-25
-10
-5
0
5
10

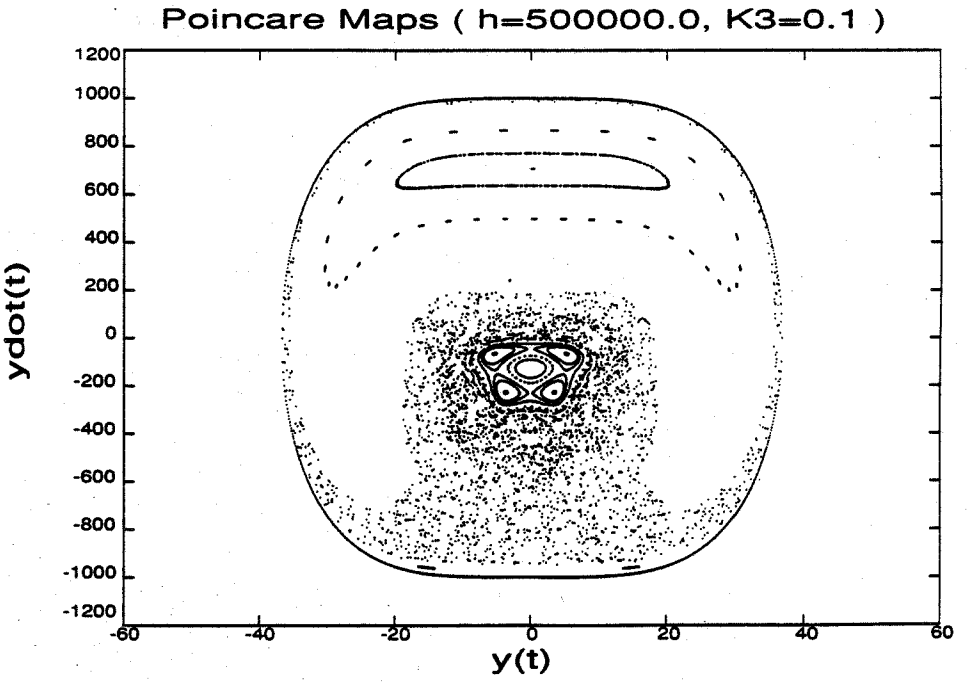
Poincare Maps (h=500000.0, K3=0.1)
ydot(t)
y(t)
1200
1000
800
600
400
200
0
-200
-400
-600
-800
-1000
-1200
-60
-40
-20
0
20
40
60

weak, a perturbation theory exists [9,11] for finding the periodic orbits of the combined system. Hence we will assume

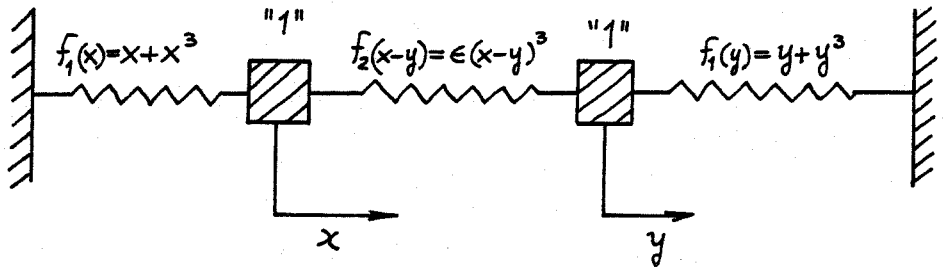

Figure 14: Weakly coupled Hamiltonian System

that the coupling spring is of perturbation order and therefore that it is proportional to a small parameter ε, $0<\varepsilon\ll 1$.

Denoting the generalised coordinates by q_1, q_2 and the generalised momenta by p_1, p_2 , from Classical Hamiltonian Theory we get:

$$q_1 = x \quad , \quad p_1 = \dot{x}$$
$$q_2 = y \quad , \quad p_2 = \dot{y} \tag{3.1}$$

and the Hamiltonian of the system can be written as:

$$H^{\varepsilon}(\underset{\sim}{p},\underset{\sim}{q}) = \underbrace{\frac{p_1^2+p_2^2}{2} + \frac{q_1^2+q_2^2}{2} + \frac{q_1^4+q_2^4}{4}}_{H^0(\underset{\sim}{p},\underset{\sim}{q})} + \underbrace{\frac{\varepsilon(q_1-q_2)^4}{4}}_{\varepsilon H^1(\underset{\sim}{p},\underset{\sim}{q})} \Rightarrow \tag{3.2}$$

$$\Rightarrow H^{\varepsilon}(\underset{\sim}{p},\underset{\sim}{q}) = H^0(\underset{\sim}{p},\underset{\sim}{q}) + \varepsilon H^1(\underset{\sim}{p},\underset{\sim}{q})$$

$$\underset{\sim}{p} \equiv (p_1,p_2), \quad \underset{\sim}{q} \equiv (q_1,q_2)$$

where we have followed the notation of [11,12] in denoting by $H^{\circ}(\underset{\sim}{p},\underset{\sim}{q})$ and $H^{\epsilon}(\underset{\sim}{p},\underset{\sim}{q})$ the unperturbed and perturbed Hamiltonians respectively and by $H^{1}(\underset{\sim}{p},\underset{\sim}{q})$ the perturbation term, containing the effect of the weak coupling. Note that for $\epsilon = 0$, the system is integrable (since it consists of two disjoint single DOF oscillatros) and thus the addition of the "coupling Hamiltonian" perturbs the integrability of the uncoupled system.

Considering the Unperturbed integrable Hamiltonian, we can express it as a sum of two Hamiltonians $F_1(q_1,p_1)$ and $F_2(q_2,p_2)$ of the uncoupled systems:

$$H^{\circ}(\underset{\sim}{p},\underset{\sim}{q}) = F_1(p_1,q_1) + F_2(p_2,q_2) \qquad (3.3)$$

where $F_i(p_i,q_i) = \frac{p_i^2}{2} + \frac{q_i^2}{2} + \frac{q_i^4}{4}$

Each of the uncoupled systems has a phase plane consisting of elliptic periodic orbits as shown in figure 15. As in [11], we

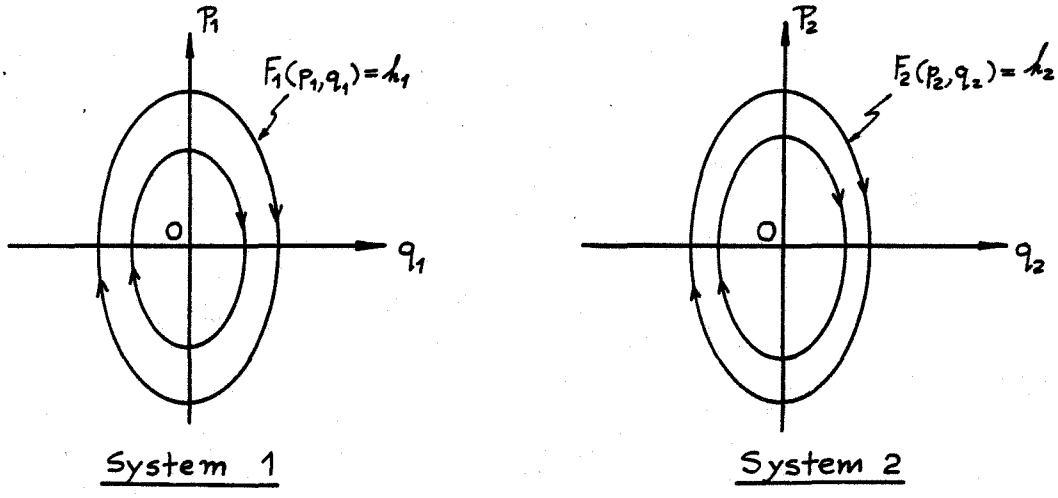

Figure 15: Phase planes of the uncoupled systems

consider the flow in the neighborhood of the elliptic periodic orbit $(0,0,q_2(t),p_2(t))$ on the energy surface $H^{\epsilon}=h$. Noting

that all the assumptions (H1 - H3) of reference [11] are satisfied for the system under consideration, it is possible to reduce the two-dimensional Hamiltonian system to the form

$$\frac{dq_1}{d\theta_2} = -\frac{\partial \mathcal{L}^0}{\partial p_1} - \varepsilon \frac{\partial \mathcal{L}^1}{\partial p_1} + O(\varepsilon^2)$$

$$\frac{dp_1}{d\theta_2} = \frac{\partial \mathcal{L}^0}{\partial q_1} + \varepsilon \frac{\partial \mathcal{L}^1}{\partial q_1} + O(\varepsilon^2) \qquad (3.4)$$

where ([11]), $\mathcal{L}^0(q_1, p_1, h) = F_2^{-1}(h - F_1(q_1, p_1))$

$$\mathcal{L}^1(q_1, p_1, \theta_2, h) = -\frac{H^1(q_1, p_1, \theta_2; \mathcal{L}^0(q_1, p_1, h))}{\Omega(\mathcal{L}^0(q_1, p_1, h))}$$

$$\Omega(I_2) = \frac{dF_2(I_2)}{dI_2}$$

and (I_2, θ_2) are the action angle variables of the uncoupled system 2.

The reduced system is of the form of the periodically perturbed planar oscillator since $\mathcal{L}^1$ has explicit dependence on the angle variable θ_2 . Thus, we can apply the Menlikov theory for subharmonic orbits developed in [4], to the study of the reduced system (3.4). Considering the (q_1, p_1, θ_2) phase space, we can find countably many resonant tori which are, direct products of the periodic orbits of the two uncoupled systems with periods T_1 and T_2 , satisfying the resonant condition

$$T_1 = \frac{m}{n} T_2 \qquad (3.5)$$

or in terms of the "time-like" variable θ_2 , the period of system 1, is

$$\bar{T}_1 = \frac{2\pi m}{n} \qquad (3.6)$$

where m, n are relatively prime positive integers. Relations (3.5), (3.6) combined with the fact that the total energy of the perturbed Hamiltonian system, is preserved, fix a unique unperturbed resonant torus for each pair (m,n).

If we now pick a point $(q_1(0), P_1(0))$ on the unperturbed level $F_1(q_1,P_1)= h_1$ of the first uncoupled oscillator and a starting time $\theta_0 \in [0,2\pi)$, the unperturbed solution based at this point is $(q_1(\theta), P_1(\theta), \theta+\theta_0)$. For this unperturbed solution, a point at θ_0

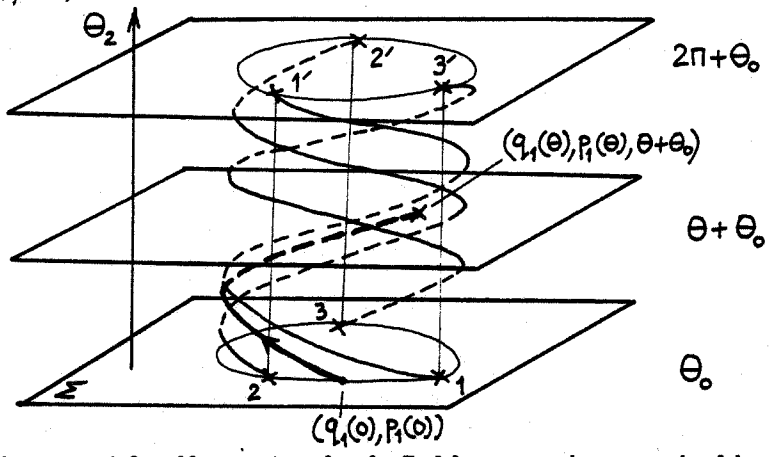

Figure 16: Unperturbed Subharmonic periodic orbit, $m/n = 3/1$.

coincides with its image at $\theta_0+2\pi m$. For the perturbed solution, we can express the distance between the initial point at θ_0 and its image at $\theta_0+2\pi m$, as:

$$d(\theta_0)= \frac{\varepsilon M(\theta_0; m,n,h)}{\| X_F(0)\|} + O(\varepsilon^2) \qquad (3.7)$$

where $X_F(0)= \left(\frac{\partial F_1}{\partial P_1} - \frac{\partial F_1}{\partial q_1}\right)\Big|_{(q_1(0),P_1(0))}$ is a normalisation factor

and $M(\theta_0,m,n,h)$ is the subharmonic Melnikov Function, given by:

$$M(\theta_0,m,n,h)=\int_0^{2\pi m}\left\{\mathcal{L}^0,\mathcal{L}^1\right\}(q_1(\theta_2-\theta_0),p_1(\theta_2-\theta_0),\theta_2,h)\,d\theta_2 \tag{3.8}$$

or in terms of time,

$$M(t_0,m,n,h)=\frac{T_2}{2\pi}\int_{-mT_2/2}^{mT_2/2}\left\{F_1,H^1\right\}(q_1(t),p_1(t),q_2(t+t_0),p_2(t+t_0))\,dt \tag{3.9}$$

where $\{.,.\}$, is the Poisson bracket [4].

We now use the following result

Theorem [Veerman, Holmes] Fix $h>0$, m, n, positive integers relatively prime and choose sufficiently small. Then if $M(\theta_0,m,n,h)$ has j simple zeros as a function of θ_0 in $[0,2\pi m/n)$ (or equivalently $M(t_0,m,n,h)$ as a function of to in $[0,T_1)$), the resonant torus given by $(q_1,p_1,\theta_2)=(q_1(\theta_2-\theta_0),p_1(\theta_2-\theta_0),\theta_2)$ breaks into $2k=j/m$ distinct $2\pi m$ - periodic orbits and there are no other $2\pi m$ periodic orbits in its neighborhood.

As pointed out in [11], this Melnikov function technique, enables us to prove the existense of only a finite number of periodic orbits in the vicinity of an unperturbed resonant torus. This is because we must let $\varepsilon\to 0$ as $m,n\to\infty$, to guarantee that the term $\varepsilon M/\|X_F\|$ dominates over the $O(\varepsilon^2)$ terms. Thus we cannot prove the existense of infinitely many periodic orbits for this system and therefore we cannot prove the nonintegrability of the system. If on the other hand, a homoclinic orbit existed in the phase plane of the unperturbed system 1, we would be able to prove an infinity of transversal homoclinic intersections for the perturbed system, via the Smale-Birkhoff homoclinic theorem.

3.2. COMPUTATIONS

3.2.1. EXISTENCE OF SUBHARMONIC ORBITS

Each of the uncoupled nonlinear Oscillator has a positive cubic nonlinearity and its unperturbed response is:

$$q_i=X_i\,cn\left([1+X_i^2]^{1/2}t/k_i\right),\quad k_i^2=\frac{X_i^2}{2(1+X_i^2)},\quad i=1,2 \tag{3.10}$$

where the following initial conditions are assumed:

$$q_i(0) = X_i \qquad (3.11)$$
$$\dot{q}_i(0) = 0$$

The amplitude of vibration X_i can be related to the energy of the uncoupled oscillator by the relation

$$X_i^2 = -1 + (1+4h_i)^{1/2} \quad , \quad h_i > 0 \qquad (3.12)$$

and hence (3.10) takes the form:

$$q_i(t) = \left(\sqrt{1+4h_i} - 1\right)^{1/2} cn\left\{(1+4h_i)^{1/4} t \,/\, k_i\right\} \quad , \quad i=1,2 \qquad (3.13)$$

where $k_i^2 = \dfrac{(1+4h_i)^{1/2} - 1}{2(1+4h_i)^{1/2}}$

The generalised momentum for system i, is given by $P_i = \dot{q}_i$ and can be computed by direct differentiation of (3.13) as:

$$P_i(t) = -(1+4h_i)^{1/4}\left(\sqrt{1+4h_i} - 1\right)^{1/2} sn\left\{(1+4h_i)^{1/4} t/k_i\right\} dn\left\{(1+4h_i)^{1/4} t/k_i\right\} \qquad (3.14)$$
$$i=1,2$$

and we have based the orbits at $(q_i(0), P_i(0)) = \left(\left\{\sqrt{1+4h_i} - 1\right\}^{1/2}, 0\right)$, $i=1,2$. For a resonance of order m/n we require that

$$nT_1 = mT_2 \Rightarrow \frac{n K(k_1)}{(1+4h_1)^{1/4}} = \frac{m K(k_2)}{(1+4h_2)^{1/4}} \qquad (3.15)$$

where $K(k_i)$ is the complete elliptic integral of the first kind and k_i is the elliptic modulus. Taking now into account

the fact that the total energy of the unperturbed resonant orbit is the sum of the energies of the two uncoupled oscillators:

$$h = h_1 + h_2 \tag{3.16}$$

we obtain:

$$\frac{nK\left[\frac{\{(1+4h_1)^{1/2}-1\}^{1/2}}{2^{1/2}(1+4h_1)^{1/4}}\right]}{(1+4h_1)^{1/4}} = \frac{mK\left[\frac{\{(1+4(h-h_1))^{1/2}-1\}^{1/2}}{2^{1/2}(1+4(h-h_1))^{1/2}}\right]}{(1+4(h-h_1))^{1/4}} \tag{3.17}$$

Now for fixed h, m and n, we will show that equation (3.17) has a unique solution for h_1 and this implies that the unperturbed system has a dense set of resonant tori in any neighborhood of the orbit $(0,0,q_2(t),P_2(t))$ on every energy level h [11].

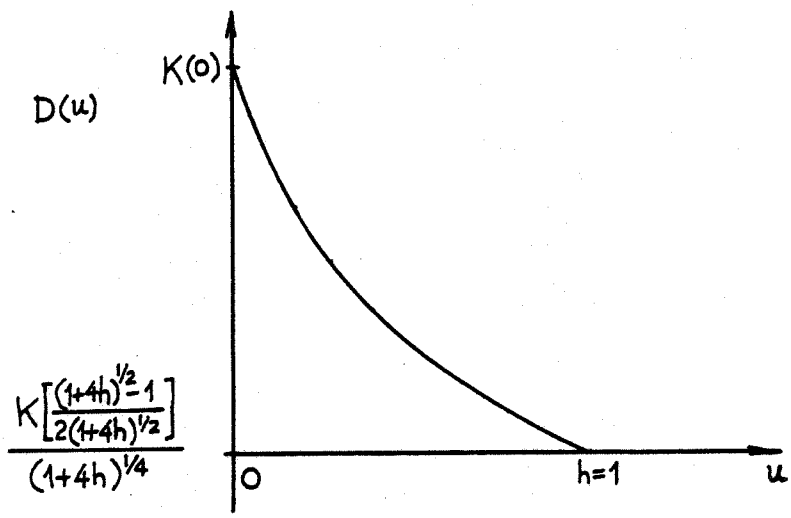

Figure 17. Plot of D(u)

To show the uniqueness of solutions for , examine the monotonicity of the quantity:

$$D(u) = K\left[\frac{\{(1+4u)^{1/2}-1\}^{1/2}}{2^{1/2}(1+4u)^{1/4}}\right] \Big/ (1+4u)^{1/4}, \quad u \in [0,h] \tag{3.18}$$

By numerical computation we can show (see figure 17), that D(u) is a monotonically decreasing function of u in the domain $u \in [0, h]$. Hence we conclude that the left hand side of equation (3.17) is monotonically decreasing, whereas the right - hand side is monotonically increasing for $h_1 \in [0, h]$ and therefore, equation (3.17) is guaranteed to have a unique solution for h_1, provided that the following inequalities are satisfied:

$$m K\left[\frac{\{(1+4h)^{1/2}-1\}^{1/2}}{2^{1/2}(1+4h)^{1/4}}\right] \Big/ (1+4h)^{1/4} \leq n K(0)$$

and

$$n K\left[\frac{\{(1+4h)^{1/2}-1\}^{1/2}}{2^{1/2}(1+4h)^{1/4}}\right] \Big/ (1+4h)^{1/4} \leq m K(0) \qquad (3.19)$$

Inequalities (3.19) pose certain restrictions on the values of m and n, and if we fix the value of h to be equal to 1, equations (3.19) give the following range for permissible values of the ratio m/n:

$$0.7241127 \leq {}^{m}/_{n} \leq 1.3810004 \qquad (3.20)$$
$$h = 1$$

Hence, only resonant orbits satisfying inequalities (3.19) are guaranteed to have a resonant torus for the fixed energy level h and is the perturbations of these orbits that we will examine in the sequence.

The Melnikov function is calculated from expression (3.9) as follows:

$$M(t_0, m, n, h) = \frac{T_2}{2\pi} \int_{-\frac{mT_2}{2}}^{\frac{mT_2}{2}} \left(\frac{\partial F_1}{\partial q_1} \frac{\partial H^1}{\partial p_1} - \frac{\partial F_1}{\partial p_1} \frac{\partial H^1}{\partial q_1} \right) \Big(q_1(t), p_1(t), q_2(t+t_0), p_2(t+t_0) \Big) dt = \qquad (3.21)$$

$$= \frac{T_2}{2\pi} \int_{-\frac{mT_2}{2}}^{\frac{mT_2}{2}} -p_1(t)\big(q_1(t) - q_2(t+t_0)\big)^3 dt$$

Now, we have to show that the equation

$$M(t_0, m, n, h) = 0 \qquad (3.22)$$

has a finite number of zeros. To this end we express (3.21) as

$$M(t_o,m,n,h)=\frac{T_2}{2\pi}\int_{-\frac{mT_2}{2}}^{\frac{mT_2}{2}}\left[-P_1(t)\,q_1^3(t)+P_1(t)\,q_2^3(t+t_o)+3P_1(t)q_1^2(t)\,q_2(t+t_o)-\right.$$

$$\left.-3P_1(t)q_1(t)q_2^2(t+t_o)\right]dt \qquad (3.23)$$

where $P_1(t)$ and $q_1(t)$ are given by expressions (3.13) and (3.14) respectivelly. But $q_1(t)$ is an even function of t and thus so is $q_1^3(t)$. To the contrary $P_1(t)$ is an odd function of t. We therefore conclude that the first term of the integral (3.23) is zero and we need only consider the remaining three terms. The period of $q_2(t+t_o)$ is T_2. Hence if we choose in (3.23), to to be:

$$t_o=\frac{kT_2}{2}=\frac{nk\,T_1}{2m}\quad,\ k \text{ positive integer} \qquad (3.24)$$

then we have that

$$q_2(t+t_o)=q_2\left(t+\frac{kT_2}{2}\right)=(-1)^k q_2(t) \qquad (3.25)$$

and for each t_o, so selected, $q_2(t+t_o)$ becomes an even function of t. Hence, recalling that $P(t)$ is an odd function of t, we conclude by (3.23), that

$$M\left(t_o=\frac{kT_2}{2},m,n,h\right)=0 \qquad (3.26)$$

k positive integer

As pointed out by Veerman, Holmes [11], computing $kn/2m$ mod. 1, for m and n relatively prime, we find precisely 2m such zeros (at $kn \bmod 2m=0,1,\ldots,2m-1$) for t_o, in the interval $0\leqslant kn/2m<1$.

Summarising, we have proven that $M_o(t_o,m,n,h)$ has 2m zeros for $0\leqslant kn/2m<1$ and we now have to prove that these zeros are simple. To prove this, we must show that

$$\left.\frac{dM_o(t_o,m,n,h)}{dt_o}\right|_{t_o=\frac{kT_2}{2}}\neq 0 \qquad (3.27)$$

Differentiating $M_o(t_o,m,n,h)$ with respect to t_o and taking into account that

$$\left.\frac{dq_2(t+t_o)}{dt_o}\right|_{t_o=\frac{kT_2}{2}} = (-1)^k \frac{dq_2(t)}{dt} \tag{3.28}$$

and that

$$P_1(t) = \frac{dq_1(t)}{dt}$$

we get the following expression for the derivative of the Subharmonic Melnikov function

$$M_o'\left(t_o=\frac{kT_2}{2}\right) = \frac{T_2}{2\pi}\int_{-\frac{mT_2}{2}}^{\frac{mT_2}{2}} \left\{(-1)^k\left[\frac{dq_2(t)}{dt}\frac{dq_1^3(t)}{dt}\right] + (-1)^k\left[\frac{dq_1(t)}{dt}\frac{dq_2^3(t)}{dt}\right] - \right. \tag{3.29}$$

$$\left. -\frac{3}{2}\left[\frac{dq_1^2(t)}{dt}\frac{dq_2^2(t)}{dt}\right]\right\} dt$$

where $(\,)' \equiv d/dt_o$

To evaluate the above expressions, we expand the functions $q_1(t)$ and $q_2(t)$ in Fourier series and evaluate the derivation appearing in (3.29) as follows (For the Fourier expansions of the elliptic cosine and its powers see Appendix A):

$$\frac{d}{dt}[q_i(t)] = \sum_{r=0}^{\infty} \Lambda_i^{(r)} \sin \gamma_i^{(r)} t \tag{3.30}$$

where $\gamma_i^{(r)} = \dfrac{(2r+1)\pi(1+4h_i)^{1/4}}{2K(k_i)}$

$$\Lambda_i^{(r)} = -\frac{\pi^2\sqrt{2(1+4h_i)}}{K^2(k_i)} \frac{(2r+1)Q_i^{r+1/2}}{1+Q_i^{2r+1}}$$

and Q_i is the elliptic nome, $Q_i = \exp\{-\pi K(1-k_i)/K(k_i)\}$ and $K(\cdot)$ is the complete elliptic integral of the first kind.

Similarly, we have that,

$$\frac{d}{dt}\left[q_i^3(t)\right] = \sum_{r=0}^{\infty} \Gamma_i^{(r)} \sin\gamma_i^{(r)} t \tag{3.31}$$

where $\gamma_i^{(r)}$ is given in expressions (3.30) and

$$\Gamma_i^{(r)} = \frac{-2^{1/2}\pi^2(1+4h_i)}{K^2(k_i)}(2r+1)\left\{2k_i^2 - 1 + (2r+1)^2\left(\frac{\pi}{2K(k_i)}\right)\right\}\frac{Q_i^{r+1/2}}{1+Q_i^{2r+1}}$$

and finally, that (3.32)

$$\frac{d}{dt}\left[q_i^2(t)\right] = \sum_{r=0}^{\infty} \Delta_i^{(r)} \cos\gamma_i^{(r)} t$$

where

$$\Delta_i^{(r)} = -\frac{2^{1/2}\pi^2(1+4h_i)}{K^2(k_i)\left(\sqrt{1+4h_i}-1\right)^{1/2}}\left[1+k_i^2 - \frac{(2r+1)^2\pi^2}{4K^2(k_i)}\right]\frac{Q_i^{r+1/2}(2r+1)}{1-Q_i^{2r+1}}$$

Before we substitute these series expressions in (3.29), we must take into account the following orthogonality condition.

$$\int_{-\frac{mT_2}{2}}^{\frac{mT_2}{2}} \cos\left[(2j+1)\frac{2\pi t}{T_1}\right]\cos\left[(2l+1)\frac{2\pi t}{T_2}\right]dt =$$

$$= \begin{cases} 0\,, \text{ if } (2j+1) \neq \dfrac{(2l+1)m}{n} \\ \dfrac{nT_1}{2} = \dfrac{mT_2}{2}\,, \text{ if } (2j+1) = \dfrac{(2l+1)m}{n} \end{cases} \tag{3.33}$$

A similar orthogonality condition holds when we have the multiplication of a sine and a cosine. So we see that the integral of (3.33) is non zero, only when,

$$(2j+1) = \frac{(2l+1)m}{n} \Longrightarrow \begin{array}{l} (2j+1) = (2\mu+1)m \\ (2l+1) = (2\mu+1)n \\ \mu = 0,1,2,\ldots \end{array} \tag{3.34}$$

Now substituting (3.30 - 3.32) into (3.29) and considering only terms satisfying (3.34), we obtain,

$$M_o'(t_o=\frac{kT_2}{2})=\frac{(-1)^k m T_2^2}{4\pi}\sum_{\mu=0}^{\infty}\left[\Lambda_2^{(\ell)}\Gamma_1^{(j)}+\Lambda_1^{(j)}\Gamma_2^{(\ell)}-\frac{3(-1)^k}{2}\Delta_1^{(j)}\Delta_2^{(\ell)}\right] \tag{3.35}$$

and j,ℓ satisfy relations (3.34).

Finally, substituring in (3.35) the expression for $\Lambda_i^{(r)}$, $\Gamma_i^{(r)}$ and $\Delta_i^{(r)}$, we get the following expression for $M_o'(t_o,m,n,h)$:

$$M'(t_o=\frac{kT_2}{2},m,n,h)=\frac{(-1)^k m}{T_1^2}\left[-256\pi^3 mn\mathcal{K}_2+1024\pi^5 mn\left(\frac{m^2}{T_1^2}+\frac{n^2}{T_2^2}\right)\mathcal{K}_4-\right.$$

$$-\frac{12(-1)^k\pi^3(1+4h_1)^{1/4}(1+4h_2)^{1/4}}{2k_1k_2}\left\{(1+k_1^2)(1+k_2^2)mn\mathcal{J}_2-\right. \tag{3.36}$$

where $$\left.\left.-(1+k_1^2)\frac{n^2\pi^2}{4K^2(k_2)}mn\mathcal{J}_4-(1+k_2^2)\frac{m^2\pi^2}{4K^2(k_1)}mn\mathcal{J}_4+\frac{m^3n^3\pi^4}{16K^2(k_1)K^2(k_2)}\mathcal{J}_6\right\}\right]$$

$$\mathcal{K}_i=\frac{1}{4}\sum_{\mu=o}^{\infty}(2\mu+1)^i\,\mathrm{sech}\left[\pi m\tau_1(\mu+1/2)\right]\mathrm{sech}\left[\pi n\tau_2(\mu+\tfrac{1}{2})\right]\ ,\ i=0,2,4$$

$$\mathcal{J}_i=\frac{1}{4}\sum_{\mu=o}^{\infty}(2\mu+1)^i\,\mathrm{csch}\left[\pi m\tau_1(\mu+1/2)\right]\mathrm{csch}\left[\pi n\tau_2(\mu+\tfrac{1}{2})\right],\ i=0,2,4,6\ ,\ \tau_i=\frac{K(1-k_i)}{K(k_i)}$$

The series expressions for $\mathcal{K}_i$ and $\mathcal{J}_i$ rapidly converge and we can have a fairly good approximation by just retaining only the first term, corresponding to $\mu=0$ (see [12] for an estimation of the involved errors, in one particular series expression). For each pair of m and n and for a fixed value of h, expresion (3.36) has to be numerically evaluated. For non zero values of $M'(t_o,m,n,h)$ we will have established the simplicity of zeros of $M(t_o,m,n,h)$ at $t_o=kT_2/2$.

Note that

$$\lim_{m,n\to\infty} M_o'(t_o=\frac{kT_2}{2},m,n,h)=0 \tag{3.37}$$

and thus this simple methodology, fails to predict subharmonic periodic orbits of all resonant tori in any neihborhood of a given torus of the elliptic orbit $(0,0,q_2(t),p_2(t))$, since this can be done only for m and n, finite. Hence, with this Melnikov approach, we can prove the existense of only a finite number of periodic orbits in the vicinity of an unperturbed resonant torus.

As a numerical example, consider an energy level $h = 1$ and a resonant torus with $m/n = 11/13$, (within the range specified by inequalities (3.20)). Equation (3.17), is solved numerically, giving

$$h_1 = 0.776$$

and thus $h_2 = h - h_1 \Rightarrow h_2 = 0.224$. These are the energy levels of the uncoupled systems, for which a resonant torus exists. Retaining only the first term of the series expressions in (3.36), we evaluate numerically the derivative of the Melnikov function at its root, as:

$$M_o'\left(t_o = \frac{kT_2}{2}\right) = \begin{cases} -5.3 \times 10^{-8}, & k = 2p \\ -5.4 \times 10^{-8}, & k = 2p+1 \end{cases}$$

and although this is a small quantity, nevertheless it is not zero. Hence we conlude that at the energy level $h = 1$, a resonant torus breaks into two distrinct $2\pi m = 22\pi$ - periodic orbits.

The resulting subharmonic periodic orbits will be discussed in the next section.

3.2.2. PHASE PLANE REPRESENTATION OF SUBHARMONIC ORBITS

To study the phase portrait of the subharmonic orbits generated in the coupled system, we have to introduce a canonical transformation of coordinates. To achieve this, consider the perturbed Hamiltonian:

$$H^{\varepsilon}(\underset{\sim}{p}, \underset{\sim}{q}) = H^{o}(\underset{\sim}{p}, \underset{\sim}{q}) + \varepsilon H^{1}(\underset{\sim}{p}, \underset{\sim}{q}) =$$

$$= F_1(q_1, P_1) + F_2(q_2, P_2) + \varepsilon \frac{(q_1 - q_2)^4}{4} \qquad (3.38)$$

where $F_i(q_i, P_i) = \frac{P_i^2}{2} + \frac{q_i^2}{2} + \frac{q_i^4}{4}$

Introduce now the following canonical transformation of coordinates:

$$(p_1, q_1) \longrightarrow (I_1, \theta_1) \tag{3.39}$$

where (I_1, θ_1) are the action-angle variables for system 1. The action variable is defined as [13]:

$$I_1(h_1) = \frac{1}{\pi}\int_{q_1^+}^{q_1^-} p_1\, dq_1 = \frac{1}{\pi}\int_{q_1^+}^{q_1^-} dq_1 \left[2(h_1 - V_1(q_1)\right]^{1/2} =$$

$$= \frac{1}{\pi}\int_{q_1^+}^{q_1^-} 2^{1/2}\left(h_1 - \frac{q_1^2}{2} - \frac{q_1^4}{4}\right)^{1/2} dq_1 \tag{3.40}$$

where $V_1(q_1)$ is the potential energy of Oscillator 1, h_1 is its total energy and the quantities $q_1^{\pm}$, represent the extremum values of the oscillation of the uncoupled system 1 (figure 18). The numerical value of $I_1(h_1)$ is given by the area enclosed by the

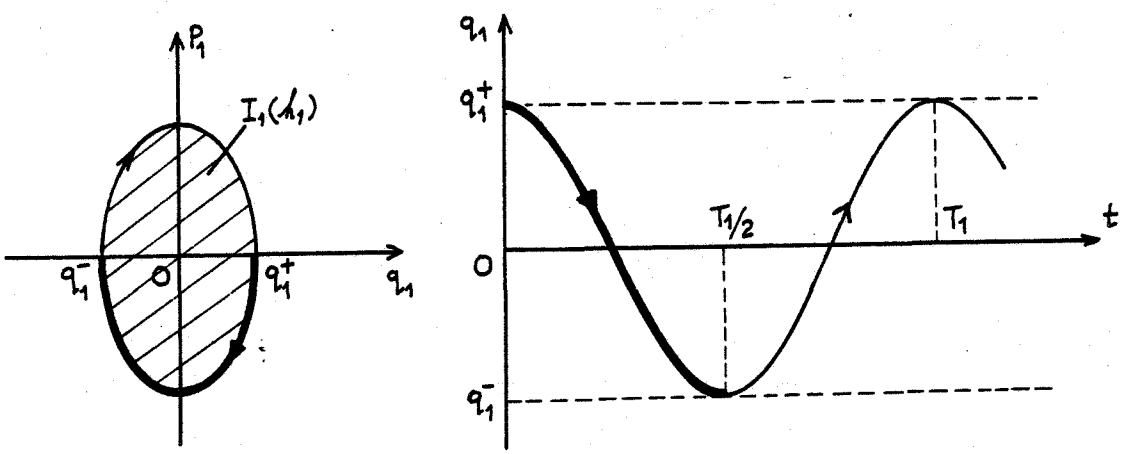

Figure 18. Path of Integration for evaluation of I_1.

free oscillation of the system in the plane. Since the expressions for $p_1(t)$ and $q_1(t)$ are already derived (expressions 3.13 - 3.14), we can directly integrate equation (3.40) as follows:

$$dq_1 = -\left(\sqrt{1+4h_1}-1\right)^{1/2}(1+4h_1)^{1/4}\,sn\left\{(1+4h_1)^{1/4}t/k_1\right\}dn\left\{(1+4h_1)^{1/4}t/k_1\right\}dt$$

and

$$I_1(h_1) = \frac{1}{\pi}\int_{q_1^+}^{q_1^-} p_1\,dq_1 = \frac{1}{\pi}\left(\sqrt{1+4h_1}-1\right)(1+4h_1)^{1/2}\int_0^{T_1/2}\left[sn^2\left\{(1+4h_1)^{1/4}t/k_1\right\}\cdot\right.$$

$$\left.\cdot\,dn^2\left\{(1+4h_1)^{1/4}t/k_1\right\}\right]dt \Rightarrow \qquad (3.41)$$

$$\Rightarrow I_1(k_1) = \frac{4}{3\pi(1-2k_1^2)^{3/2}}\left[E(k_1)(2k_1^2-1)+k_1'^2K(k_1)\right]$$

where $K(\cdot)$ and $E(\cdot)$ are the complete elliptic integrals of first and second kind respectively, and $k_1'^2 = 1-k_1^2$. Note that in (3.41) I_1 is related implicitly with the old coordinates (p_1,q_1) and the energy h_1 , since k_1 satisfies the expressions

$$h_1 = \frac{p_1^2}{2}+\frac{q_1^2}{2}+\frac{q_1^4}{4} = \frac{1}{4}\left[\frac{1}{(1-2k_1^2)^2}-1\right] \qquad (3.42)$$

The angle variable θ_1 is computed by expressions given in [13] and we will not give explicit expressions for it, since this is not needed for what follows.

Consider now the reduced system of equations (3.4):

$$\frac{dq_1}{d\theta_2} = -\frac{\partial\mathcal{L}^0}{\partial p_1}-\varepsilon\frac{\partial\mathcal{L}^1}{\partial p_1}+O(\varepsilon^2)$$

$$\frac{dp_1}{d\theta_2} = \frac{\partial\mathcal{L}^0}{\partial q_1}+\varepsilon\frac{\partial\mathcal{L}^1}{\partial q_1}+O(\varepsilon^2) \qquad (3.4)$$

Note that Θ_2 is a "time-like" variable and for $\varepsilon = 0$, the unperturbed system is Hamiltonian with Hamiltonian $\mathcal{L}^\circ$. Now introduce the action angle trasformation of (3.39) into the reduced system (3.4). By symbolically writting:

$$I_1 = I_1(p_1, q_1) \quad , \quad p_1 = p_1(I_1, \Theta_1)$$
$$\Theta_1 = \Theta_1(p_1, q_1) \quad , \quad q_1 = q_1(I_1, \Theta_1) \tag{3.43}$$

and substituting for q_1, p_1 in the expressions for $\mathcal{L}^\circ$ and $\mathcal{L}^1$, we get:

$$\mathcal{L}^\circ(q_1, p_1, h) = \mathcal{L}^\circ(q_1(I_1,\Theta_1), p_1(I_1,\Theta_1), h) \equiv \hat{\mathcal{L}}_\circ(I_1, h)$$
$$\mathcal{L}^1(q_1, p_1, \Theta_2) = \mathcal{L}^1(q_1(I_1,\Theta_1), p_1(I_1,\Theta_1), \Theta_2) \equiv \hat{\mathcal{L}}_1(I_1, \Theta_1, \Theta_2) \tag{3.44}$$

Note that there is no explicit dependence of $\hat{\mathcal{L}}_\circ$ on Θ_1, since (I_1, Θ_1) are the action angle variables of the unperturbed system [13].

Now we can symbolically transform the reduced system into the new variables as follows [11]:

$$\frac{dI_1}{d\Theta_2} = \varepsilon \frac{\partial \hat{\mathcal{L}}_1(I_1,\Theta_1,\Theta_2)}{\partial \Theta_1} + O(\varepsilon^2)$$
$$\frac{d\Theta_1}{d\Theta_2} = -\omega(I_1) - \varepsilon \frac{\partial \hat{\mathcal{L}}_1(I_1,\Theta_1,\Theta_2)}{\partial I_1} + O(\varepsilon^2) \tag{3.45}$$

where $\omega(I_1) = d\hat{\mathcal{L}}_\circ(I_1) / dI_1$ and we have omitted the dependence of $\hat{\mathcal{L}}_\circ$ on the total energy h.

Consider now the unperturbed orbit corresponding to the resonance $m T_2 = n T_1$. This orbit is given by (set $\varepsilon = 0$, in (3.45)):

$$I_1 = \overline{I}_1$$
$$\Theta_1 = -\omega(I_1)\Theta_2 = -\frac{n}{m}\Theta_2 \tag{3.46}$$

Consider now small perturbations from this unperturbed orbit [11,12]:

$$I_1 = \bar{I}_1 + \sqrt{\varepsilon} K$$
$$\theta_1 = -\frac{n}{m}\theta_2 + \psi \qquad (3.47)$$

Substituting (3.47) into the reduced system (3.45), we get the following variational equations for K and ψ :

$$\frac{dK}{d\theta_2} = \sqrt{\varepsilon}\frac{\partial \hat{\mathcal{L}}_1(\bar{I}_1, -\frac{n\theta_2}{m}+\psi, \theta_2)}{\partial \theta_1} + \varepsilon \frac{\partial \hat{\mathcal{L}}_1(\bar{I}_1, -\frac{n\theta_2}{m}+\psi, \theta_2)}{\partial I_1} K + O(\varepsilon^{3/2})$$
$$\frac{d\psi}{d\theta_2} = -\sqrt{\varepsilon}\frac{d\omega(\bar{I}_1)}{dI_1} K - \varepsilon\left[\frac{\partial^2 \hat{\mathcal{L}}_1(\bar{I}_1, -\frac{n\theta_2}{m}+\psi, \theta_2)}{\partial I_1^2} + \frac{d^2\omega(\bar{I}_1)}{dI_1^2}\frac{K^2}{2}\right] + O(\varepsilon^{3/2}) \qquad (3.48)$$

Following the methodology presented in [11,12,14], we apply the averaging theorem and for $\sqrt{\varepsilon}$ sufficiently small, we can remove the explicit "fast" variable θ_2 dependence from (3.48), obtaining the following averaged variational equations:

$$\frac{d\bar{K}}{d\theta_2} = \frac{\sqrt{\varepsilon}}{2\pi n} M\left(\frac{\bar{\psi}}{\omega(\bar{I}_1)}\right)$$
$$\frac{d\bar{\psi}}{d\theta_2} = -\sqrt{\varepsilon}\frac{d\omega(\bar{I}_1)}{dI_1}\bar{K} \qquad (3.49)$$

and $M(\bar{\psi}/\omega(\bar{I}_1))$ is the same Subharmonic Melnikov function encountered previously, the only difference being that the independent variable is $\bar{\psi}/\omega(\bar{I}_1)$ instead of t_o .

Under the Averaging theorem, the hyperbolic and elliptic fixed points of (3.49) correspond to small periodic motions of the variations described by (3.48) and therefore to subharmonics of order m/n of the reduced system (3.45). As in the previous section, a necessary and sufficient condition for the existence of such fixed points for (3.49), is that the Subharmonic Melnikov function have simple zeros and that $\omega(I_1) \neq 0$.

Furthermore, as pointed in the aforementioned references, the averaged system (3.49) is Hamiltonian with Hamiltonian function given by:

$$H(\bar{K},\bar{\psi})=\sqrt{\varepsilon}\left[\frac{d\omega(\bar{I}_1)}{dI_1}\frac{\bar{K}^2}{2}+\int_0^{\bar{\psi}}\frac{1}{2\pi n}M\left(\frac{\eta}{\omega(\bar{I}_1)}\right)d\eta\right] \tag{3.50}$$

and the maximum separation of the level curves of H which contain hyperbolic fixed points is given by:

$$K_{max}=\left\{\frac{2}{\frac{d\omega(\bar{I}_1)}{dI_1}}\max_{\bar{\psi}\in[0,2\pi)}\left(\int_0^{\bar{\psi}}\frac{1}{2\pi n}M\left(\frac{\eta}{\omega(\bar{I}_1)}\right)d\eta\right)\right\}^{1/2} \tag{3.51}$$

Using (3.51), one can estimate the bandwidth of different resonant bands and calculate the maximum "island widths" in the Poincaré Map as $\sqrt{\varepsilon}K_{max}$. For such a detailed work, see [12].

We will now apply the above methodology to the case of the coupled two-degree-of-freedom system considered in this work. The expression for the Melnikov function was given in the previous section and the only unknown quantity in the averaged variational equations (3.49), is $d\omega(\bar{I}_1)/dI_1$. To compute this quantity, we express it as [14]:

$$\frac{d\omega(\bar{I}_1)}{dI_1}=\frac{d}{dI_1}\left(\frac{2\pi}{T_1(I_1)}\right)_{I_1=\bar{I}_1} \tag{3.52}$$

and considering I_1 as a function of k_1, $I_1=I_1(k_1)$, we write the above expression as:

$$\frac{d\omega(\bar{I}_1)}{dI_1}=-\frac{\left(2\pi/T_1(\bar{I}_1)^2\right)\frac{dT_1(k_1)}{dk_1}}{\frac{d}{dk_1}I_1(k_1)} \tag{3.53}$$

where $T_1(k_1)=4K(k_1)/(1+4h_1)^{1/4}$. Using the relation $h_1=\frac{1}{4}\left[\frac{1}{(1-2k_1^2)^2}-1\right]$ we get an expression for $T_1^2(I_1)$ as follows:

$$T_1^2(\bar{I}_1)=16K^2(k_1)(1-2k_1^2) \tag{3.54}$$

Differentiating the expression for $T_1 = T_1(k_1)$ with respect to k_1, we obtain

$$\frac{dT_1(k_1)}{dk_1} = \frac{4E(k_1)(1-2k_1^2) - K(k_1)(1-k_1^2)}{k_1(1-k_1^2)(1-2k_1^2)^{1/2}} \tag{3.55}$$

and differentiating expression (3.41) of $I_1 = I_1(k_1)$ with respect to k_1,

$$\frac{dI_1(k_1)}{dk_1} = \frac{4K(k_1)\,k_1}{\pi(1-2k_1^2)^{5/2}} \tag{3.56}$$

Finally, combining expressions (3.53 - 3.56), we derive the following formula for $d\omega(\bar{I}_1)/dI_1$:

$$\frac{d\omega(\bar{I}_1)}{dI_1} = -\frac{\pi^2\left[E(k_1)(1-2k_1^2) - K(k_1)(1-k_1^2)\right](1-2k_1^2)}{8K^3(k_1)\,k_1^2(1-k_1^2)} \tag{3.57}$$

So, the right hand sides of the set of the averaged variational equations (3.49) are known. As far as the Melnikov function is concerned, we have proved in the previous section, the existense of 2m simple zeros. Also, by considering the above expression for $d\omega(\bar{I}_1)/dI_1$, we have that

$$1-2k_1^2 > 0 \quad \text{for } h_1 > 0 \tag{3.58}$$

since as $h_1 \to \infty$, $k_1^2 \to 1/2$, and for all other values of h_1, $k_1^2 < 1/2$.

Furthermore, it is satisfied that

$$E(k_1)(1-2k_1^2) - K(k_1)(1-k_1^2) < E(k_1)(1-k_1^2) - K(k_1)(1-k_1^2) < \leqslant (E(k_1) - K(k_1))(1-k_1^2) < 0 \tag{3.59}$$

since $E(k)-K(k)<0$ and $1-k_1^2>0$. Combining (3.58) and (3.59) we have that

$$\frac{d\omega(\bar{I}_1)}{dI_1} > 0 \tag{3.60}$$

and as a consequence $d\bar{\psi}/d\theta_2 < 0$ in equations (3.49) and the averaged phase portrait rotates counterclockwise.

From the above, we conclude that the $(\bar{K}, \bar{\psi})$ phase portrait of the averaged variational equations (3.49) must look as in figure 19, where the zeros for $\bar{K}$ correspond to the zeros of the Melnikov function $M(\bar{\psi}/\omega(\bar{I}_1))$. The maximum "island" width can

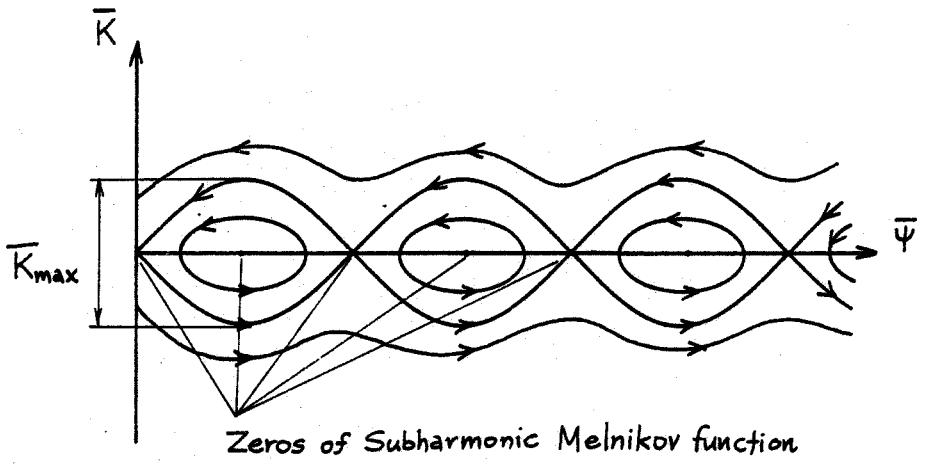

Figure 19: Phase plane of the averaged variation equations (3.49)

be estimated by expression (3.51). In the (q_1, p_1) plane, the phase portrait looks as in Figure 20. Note that this is how the level curves of the averaged Hamiltonian system appear. The elliptic and hyperbolic points alternate and the averaging theorem does not guarantee that the families of heteroclinic orbits connecting the hyperbolic points are preserved as smooth manifolds. Rather one expects the stable and unstable manifolds

to intersect transversely, but this cannot be proven by Melnikov-type arguments, since the Melnikov functions involved is exponentially small [11]. If such transverse intersections were proven to occur, then one would be able to prove the non existense of analytic second integrals of motion for the coupled system (as for systems where transverse homoclinic intersections occur).

Concluding this section, we note that with this Melnikov technique we are able to identify "primary islands" [8] of resonance bands, such as those observed in the Poincaré Plots of figures 13 of the previous section. Furthermore, by introducting new canonical transformations and rescaling, one could predict "secondary" islands, within the primary islands of figure 20. However by this type of arguments it is not possible to model the ergodic motion ("sea of stochasticity") taking place within the preserved irrational KAM tori of figures 13.

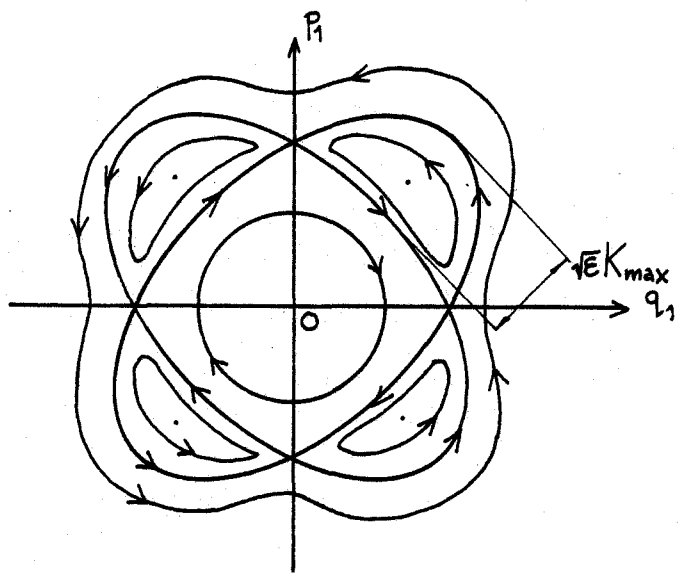

Figure 20. Resonant Bands (after Veerman-Holmes[11]).

4. FORCED OSCILLATIONS OF THE NONLINEAR SYSTEM

In this section we will examine the exact steady state forced vibrations of the two degree of freedom oscillator. Definitions for steady state motions are given in [1] and will not be repeated here. We will examine two separate categories of systems, namely systems that possess additional modes of free oscillation and systems that only have the symmetric and antisymmetric modes. In the former case, we will observe an interesting phenomenon: The topological portrait of the resonance curves changes, when we vary the numerical value of a structural parameter of the system. To the contrary, no such phenomenon exists for systems with only two modes of free oscillation. In a final section we will use perturbation analysis to demonstrate that the exact steady states described here degenerate to approximate harmonic solutions, when the nonlinearities and/or the amplitudes of motion are of perturbation order.

4.1. SYSTEMS WITH ADDITIONAL MODES OF FREE OSCILLATION

Consider the forced system of figure 21. A periodic (but not necessarely harmonic) force acts on the left mass, and as previously , we assume that the two masses are equal to the unit mass and that the potential function of the system is positive definite and symmetric with respect to the origin in the configuration space. For convenience, the system is assumed to be symmetric, but the same analysis can be performed for an unsymmetric system. The dependence of the stiffness on the amplitude is given by the following expressions:

$$f_i(u) = \sum_{k=1,3,5,\ldots} f_{ik}\, u^k \quad , \quad i = 1,2,3 \qquad (4.1)$$

$$f_{1k} = f_{3k} \quad , \quad k = 1,3,5,\ldots$$

Again we will assume that $f_{ik} > 0$ and cases when this does not hold are treated similarly.

According to Rosenberg's definition [2], the steady state of a Multi-Degree-of-Freedom System under a periodic forcing, is a motion in which all masses vibrate "in unison" and the period of the responce is the same with that of the forcing. The basic question concerning the steady state problem is: Given a prescribed set of initial conditions of the system, what should be the form of the excitation $p(t)$, leading to a steady state motion?

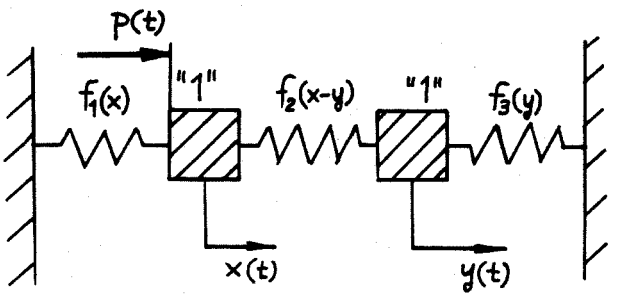

Figure 21. The Forced system

To answer this question, we consider first the linear case:

$$f_1(u) = k_1 u$$
$$f_2(u) = k_2 u \qquad (4.2)$$
$$f_3(u) = k_1 u$$

Now, for the set of initial conditions $x(0)=X$, $\dot{x}(0)=0$, $y(0)=Y$, $\dot{y}(0)=0$, we get the following steady-state harmonic responce.

$$x(t) = X\cos\omega t$$
$$y(t) = c\,x(t) \qquad (4.3)$$
$$P(t) = \tilde{P}(x(t)) = \frac{P}{X}\,x(t) = P\cos\omega t$$

where

$$\omega^2 = k_1^2 - k_2^2\,\frac{(1-c)}{c}$$
$$P/X = k_1^2 + k_2^2(1-c) - \omega^2 \qquad (4.4)$$
$$Y = cX$$

The steady state solution is commonly studied by the response curves of figure 22 (or resonance curves) and because of linearity, all solutions are orbitally stable. We note from the harmonic steady state, that the forcing function is related to the steady state displacement $x(t)$ by a certain functional relation $\tilde{P}(\cdot)$, linear in this case. Another feature of the solution, is that at the steady state, the two differential equations of motion are uncoupled and the two displacements $y(t)$ and $x(t)$ are related linearly to each other for all times.

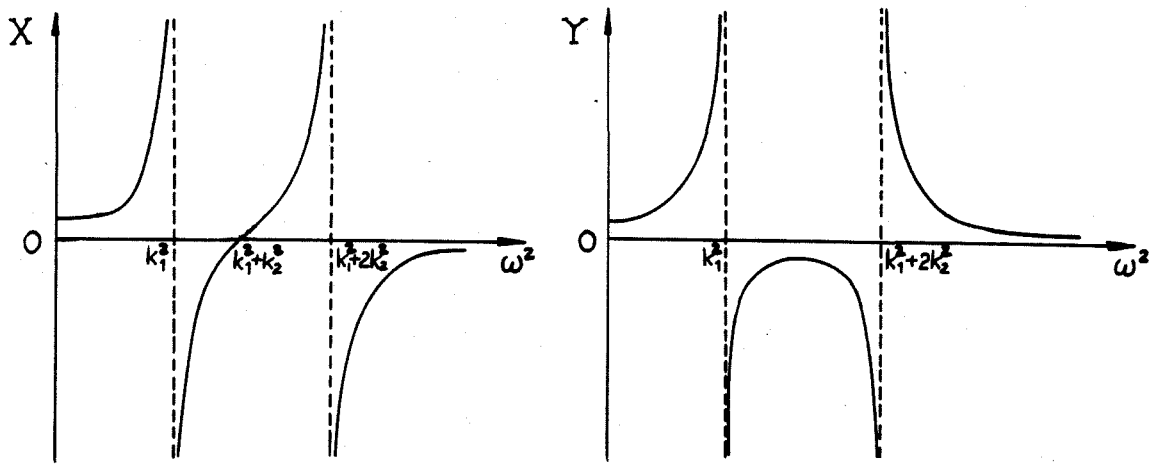

Figure 22. Response curves for the Linear System

From the above we conclude, that to extend the motion of the "steady state" to nonlinear systems, it is natural to require that for such motions to occur, the forcing $p(t)$ and the displacements $x(t), y(t)$ should be related by expressions of the form [2,15]:

$$p(t) = \tilde{p}(x(t))$$
$$y(t) = c\,x(t) \tag{4.5}$$

where c is assumed to be a constant scalar. Then, to obtain the steady state motion, we have to determine the form of $\tilde{p}(\cdot)$ and the values of c that uncouple the equations of motion for a prescribed set of initial conditions.

Consider now the nonlinear forced system of figure 21. The free oscillations of this system were investigated in [1] for the symmetric case and in the first section of this work for the unsymmetric one. It was shown that the symmetric system always posseses the symmetric and anti-symmetric modes, where the masses vibrate in-phase or out-of-phase for all times:

$$y(t) = x(t) \quad (\text{Symmetric mode})$$
$$y(t) = -x(t) \quad (\text{Antisymmetric mode}) \tag{4.6}$$

However, it was also found that the nonlinear system can posses additional normal modes (in direct contrast to the linear case) and a condition for their existense was that the coupling spring does not contain any linear part [1]. If this condition is

satisfied, additional modes can exist and they are conveniently studied by means of the "Balancing Diagrams" of the nonlinearities present in the system. We will start the steady state analysis by considering a symmetric system with additional modes, and in the next section, we will generalise the methodology by examining systems with no additional modes of free oscillation.

To this end, we assume that the coupling spring $f_2(u)$, does not contain a linear part and that the nonlinearities are of order k :

$$\begin{aligned} f_1(u) &= f_{11}u + f_{1k}u^k \\ f_2(u) &= f_{2k}u^k \\ f_3(u) &= f_1(u) \end{aligned} \tag{4.7}$$

where k is odd and $f_{ij}>0$. It was shown in [1], that depending on the ratio $r = f_{2k}/f_{1k}$, this system can have more than two modes of free oscillation. Assuming the set of initial conditions

$$\begin{aligned} x(0) &= X \quad , \quad y(0) = Y \\ \dot{x}(0) &= 0 \quad , \quad \dot{y}(0) = 0 \end{aligned} \tag{4.8}$$

we inquire about the form of the forcing function necessary for a steady state motion. Assuming as in [2,16] a form:

$$P(t) = \tilde{P}(x(t)) = \left(\frac{P}{X}\right)^k x^k(t) \tag{4.9}$$

the differential equations of motion of the system become

$$\begin{aligned} \ddot{x} + f_{11}x + f_{1k}x^k + f_{2k}(x-y)^k &= \left(P/X\right)^k x^k \\ \ddot{y} + f_{11}y + f_{1k}y^k + f_{2k}(y-x)^k &= 0 \end{aligned} \tag{4.10}$$

At the steady state, the displacements should be related by $y(t) = cx(t)$ for all times and substituting for $y(t)$ into the equations of motion , we obtain:

$$\begin{aligned} \ddot{x} + f_{11}x + \left[f_{1k} + f_{2k}(1-c)^k - \left(\frac{P}{X}\right)^k \right] x^k &= 0 \\ \ddot{x} + f_{11}x + \left[f_{1k}c^2 - f_{2k}\,\frac{(1-c)^k}{c} \right] x^k &= 0 \end{aligned} \tag{4.11}$$

These equations have to be solved with the set of initial conditions (4.8), with $Y = cX$.

From equation (4.11) we see that the forced problem is transformed to a free vibration one. Each of equations (4.11) is a differential equation in $x(t)$ and has to be solved with the same set of initial conditions. It is evident that the condition for exact steady state, is that both equations give the same solution for X (i.e. the two differential equations become identical) and therefore that the coefficients of the respective powers of $x(t)$ must be equal. We see that for this system, the linear terms are identical for every value of c (this does not hold when the coupling spring contain a linear term) and we therefore conclude that for a steady state motion, it must be satisfied that:

$$f_{1k} + f_{2k}(1-c)^k - \left(\frac{P}{X}\right)^k = f_{1k}c^{k-1} - f_{2k}\frac{(1-c)^k}{c} = \mu_k \qquad (4.12)$$

For a given initial amplitude X and a force magnitude P, we compute c from (4.12), $x(t)$ from any of equations (4.11) and $y(t)$ from the modal relation $y(t) = cx(t)$. General expressions for the solution of equations (4.11) can be found in [1] and from the same reference, we use the following formula to compute the frequency of oscillation at the steady state:

$$\omega = \omega(X,P) = \frac{\pi \Omega^{1/2}}{2\int_0^{\pi/2}\left[1 + \frac{2\mu_k X^{k-1} V_k(\varphi)}{(k+1)\Omega}\right]^{-1/2} d\varphi} \qquad (4.13)$$

where $$V_k(\varphi) = \frac{1-\cos^{k+1}(\varphi)}{1-\cos^2(\varphi)}$$

$$\Omega = \Omega(X,P) = f_{11} + \frac{2\mu_k}{k+1}X^{k-1}$$

Expression (4.13) relates the amplitude X to the frequency of oscillation ω for a fixed value of the forcing P and

therefore, (4.13) gives the response curves of the system, in direct analogy to the linear response (resonance) curves of figure 22. Note that if we set $P=0$, expression (4.13) gives the backbone curves of free oscillation and the corresponding free oscillation values for c are found from (4.12) with $P=0$;

$$f_{1k}+f_{2k}(1-c)^k = f_{1k}c^{k-1} - f_{2k}\frac{(1-c)^k}{c} \qquad (4.14)$$

As shown in [1], this equation has always the solutions $c=\pm 1$ (corresponding to the symmetric and antisymmetric modes) and depending on the ratio $r=f_{2k}/f_{1k}$, additional real roots for c are possible (corresponding to additional modes). We therefore conclude, that by varying the value of the structural paramenter r , we can change the number of backbone curves of the system and thus invoke changes in the topological portrait of the response curves (4.13). This fact will be demonstrated with an application later.

From the above, it is clear that the necessary forcing $p(t)$ for the occurence of the steady state motion, is given by the form (4.9). In addition it can be shown that this is the only forcing capable of producing a steady state for the symmetric system with stiffness given by expressions(4.7). An interesting feature of the analysis, is that the coefficient of the linear terms f_{11} plays no essential role in the determination of $p(t)$ or in the topology of the response curves.

In [16], a Geometrical method in the configuration plane was used to study the steady state motion of the "Homogeneous" system, i.e. the system with all stiffnesses proportional to the same power of the displacement. The system was excited by a cam-function and the response was expressed in terms of a generalised frequency λ . The results obtained in this work are equivalent to those reported in [16], if one relates the generalised frequency λ , and the variable μ_k of equation (4.12), by:

$$\mu_k = \lambda^2 c^{k-1}$$

However, our analysis is slightly more general in the sense that we do not require homogenuity in the stiffnesses (in our analysis $f_{11}\neq 0$). We finally note that an approximate analysis of the same Homogeneous system with cubic nonlinearities was carried out by Szemplinska - Stupnica [17] and the approximate harmonic response of the system near resonances was obtained.

As an application of the aforementioned theory, we consider the case when $k=3$ (cubic nonlinearities). In this case, equation (4.12) takes the form:

$$f_{13}+f_{23}(1-c)^3 - \left(\frac{P}{X}\right)^3 = f_{13}c^2 - f_{23}\frac{(1-c)^3}{c} = \mu_3 \qquad (4.15)$$

The relation between μ_3 and the quantity P/X, can be found by eliminating c from equations (4.15):

$$\mu_3 = f_{13}\left[1-\left\{\frac{\mu_3}{f_{23}}+\frac{1}{f_{23}}\left(\frac{P}{X}\right)^3-\frac{f_{13}}{f_{23}}\right\}^{1/3}\right]^2-\frac{\mu_3+\left(\frac{P}{X}\right)^3-f_{13}}{1-\left\{\frac{\mu_3}{f_{23}}+\frac{1}{f_{23}}\left(\frac{P}{X}\right)^3-\frac{f_{13}}{f_{23}}\right\}^{1/3}} \quad (4.16)$$

By fixing the value of the forcing P and for each value of the amplitude X, μ_3 can be computed by numerically solving the above equation. Then c can be computed from any one of equations (4.16).

Equations (4.11) combined with initial conditions (4.8), lead to the following expression for the displacement x at the steady state:

$$x(t) = X\,cn\left(\left[f_{11}+\mu_3 X^2\right]^{1/2} t/k_1\right) \quad , \quad \mu_3 > 0$$

$$x(t) = X\,sn\left(\left[f_{11}+\mu_3 X^2/2\right]^{1/2} t/k_2\right) \quad , \quad 0 > \frac{\mu_3 X^2}{f_{11}} > -1 \qquad (4.17)$$

where k_1, k_2 are the elliptic moduli, given by

$$k_1^2 = \frac{\mu_3 X^2}{2\left(f_{11}+\mu_3 X^2\right)} \quad , \quad k_2^2 = \frac{-\mu_3 X^2}{2f_{11}+\mu_3 X^2}$$

Note that in the above solution, we have excluded the possibility of unbounded motion corresponging to values of μ_3 such that $\mu_3 X^2/f_{11} < -1$. This is because as we will show later, such motions cannot be realised in the system under consideration. The response curves at the steady state are found by (4.13) by setting $k=3$:

$$\omega = \frac{\pi\left(f_{11}+\mu_3 X^2\right)^{1/2}}{2K(k_1)} \quad , \quad \mu_3 > 0$$

$$\omega = \frac{\pi\left(f_{11}+\mu_3 X^2/2\right)^{1/2}}{2K(k_2)} \quad , \quad 0 > \frac{\mu_3 X^2}{f_{11}} > -1 \qquad (4.18)$$

where $K(\cdot)$ is the complete elliptic integral of the first kind and μ_3 is computed from equations (4.15).

In figure 23, the roots c of equations (4.15) are schematically plotted against the structural parameter $r = f_{23}/f_{13}$ for fixed forcing P and amplitude X. These diagrams represent the

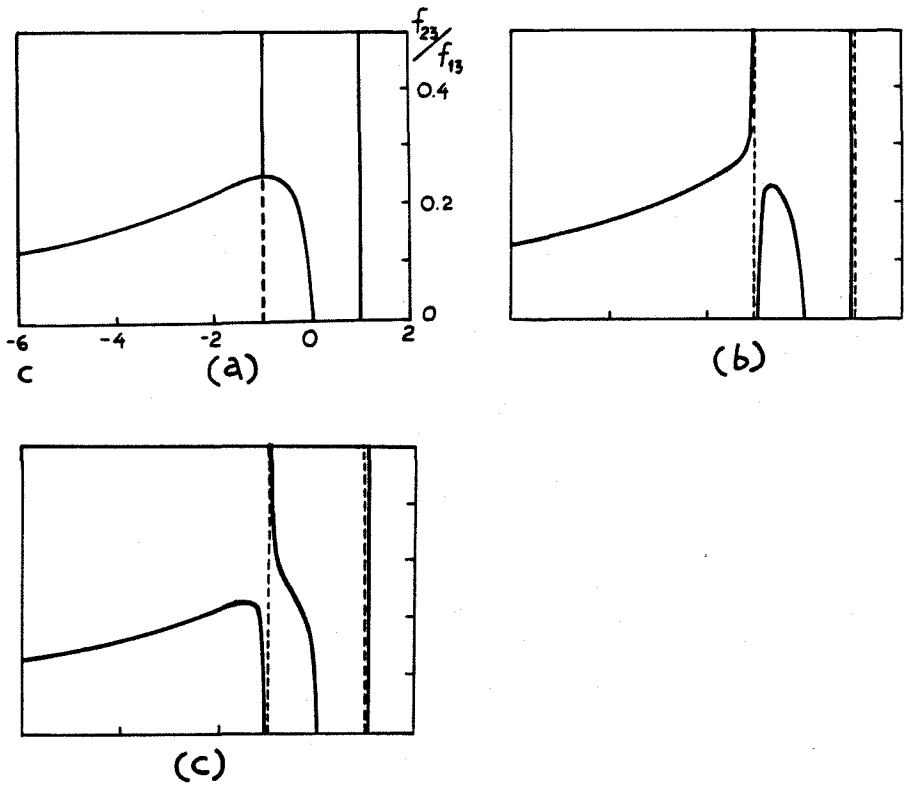

Figure 23. Balancing Diagrams of the system with cubic nonlinearities: (a) $P=0$, (b) $P/X>0$ (c) $P/X<0$.

balancing of the cubic nonlinear terms in the system and note that since the coupling spring contains no linear term, no Linear Balancing Diagram exists. Figure 23(a) gives the modes of free oscillation and we see that at $r = 1/4$, a Hamiltonian Pitchfork Bifurcation occurs and the antisymmetric mode exchanges stability, becoming orbitally unstable.

This means that the symmetric system under consideration can have two or four backbone curves (of which one represents orbitally unstable free oscillations), depending on the value of the ratio r of the coefficients of the cubic terms of the springs.

When a forcing $P \neq 0$ is applied, we see form figures 23(b,c) that the pitchfork bifurcation breaks and c now denotes the value of the modal parameter at the steady state. For values of r larger than 1/4, we can have at most two such values of c, whereas for r less than 1/4, four values for c exist. From this observation we have a first indication that the topological portrait of the repsonse curves differs for values of r greater or less than 1/4 and this is a direct consequense of the fact that additional normal modes exist for this system.

In figures 24 and 25, we present the Amplitude-Frequency response curves for two forced symmetric systems. In both cases the forcing was set equal to $P=0.5$ and the structural parameters were chosen to be $f_{11} = f_{13} = 1.0$. For the first system the ratio of the cubic nonlinearities was set equal to $r=0.4$, whereas for the second we used the value $r=0.15$, to demonstrate the difference in the topology of the response curves for the two systems. To construct these curves, we first assigned fixed values for the initial conditions and consequently computed c and μ_3 from (4.15) and ω from (4.17).

We see from figure 24, that at most five steady states exist of which only three are orbitally stable. However, by setting the parameter r below 1/4, we observe from figure 25 that the possible steady sttes were increased to nine, of which only four are orbitally stable. The stability analysis was carried out by means of the approximate method presented in [16] and details of it can be found in Appendix B. At this point it must be emphasised that by the term "stability" we mean orbital stability and not Liapunov stability which is not possible for the class of systems considered in this work. An interesting remark on the response curves of figure 25, is that all steady states neighboring the orbitally unstable backbone curve (representing the unstable antisymmetric mode), are also orbitally unstable and this tells us that no stable steady can result in the vicinity of an orbitally unstable free oscillation. Finally we note that since no damping is present in our models, the phases of the steady states can only be 0 or 180° (this can be also observed in the linear undamped responses of figure 22).

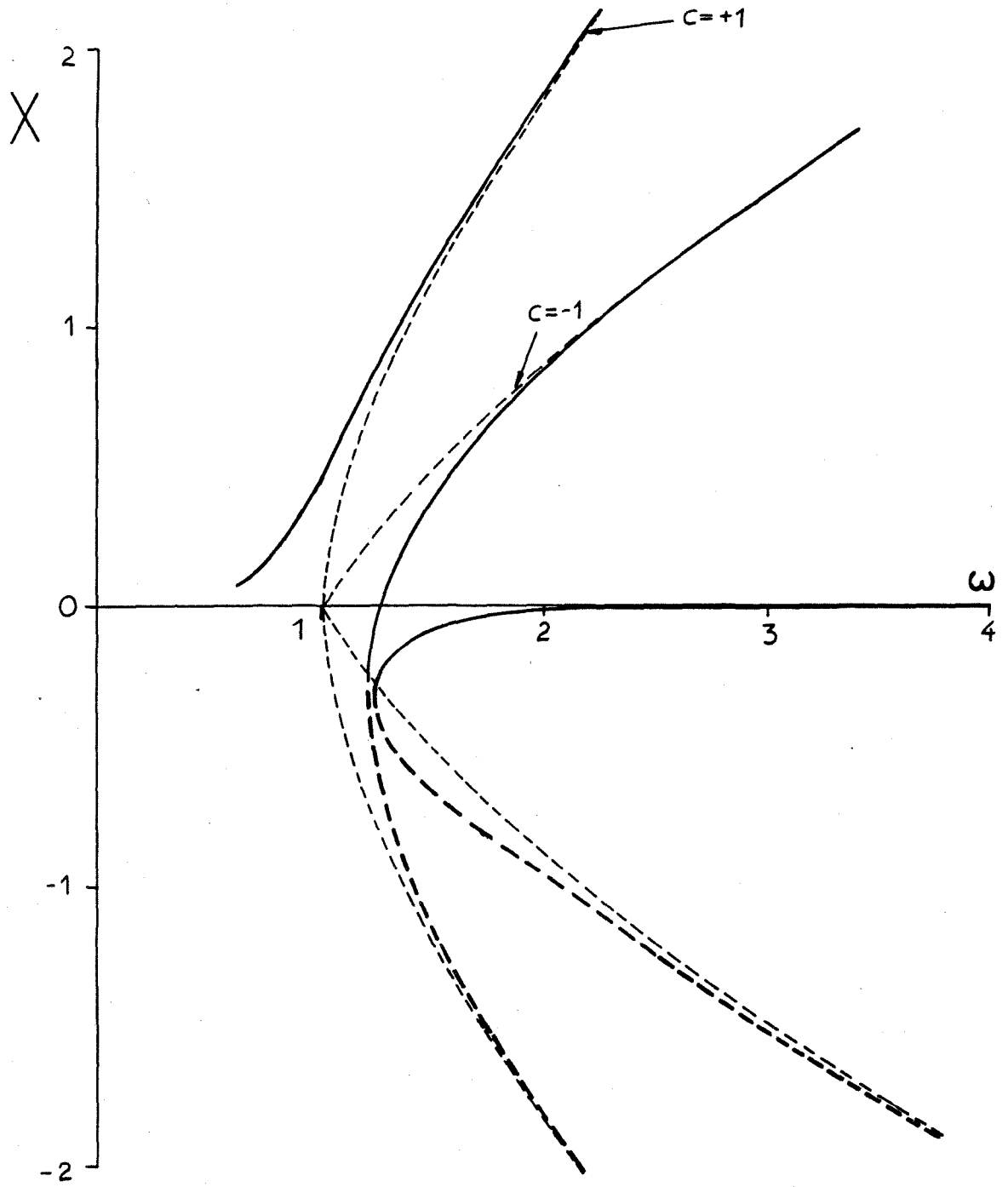

Figure 24. Response curves of the symmetric system for $r = 0.4 > 1/4$
Stable solutios _____,
unstable solutions ----------

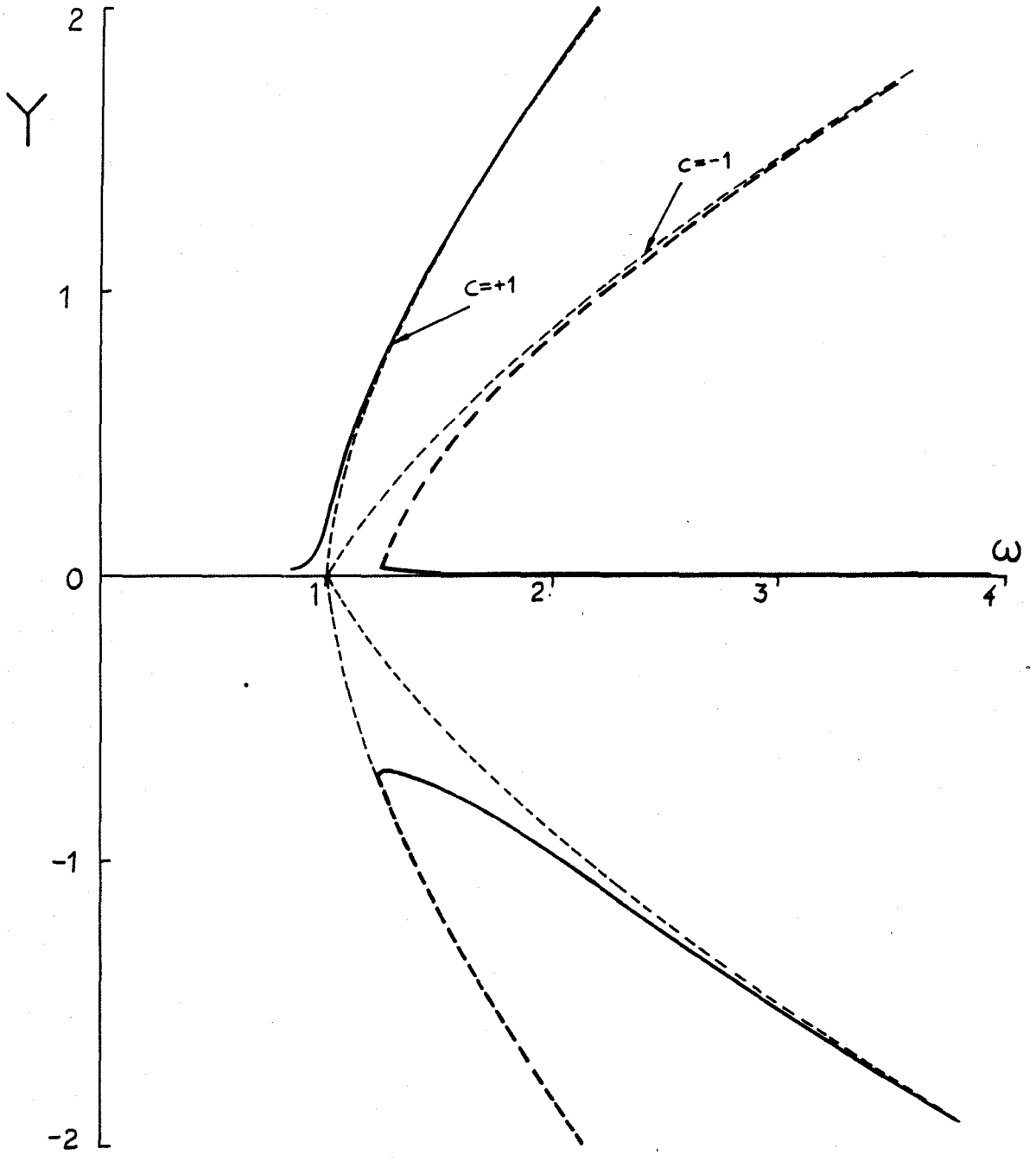
2
Y
1
0
-1
-2
C=-1
C=+1
ω
1
2
3
4

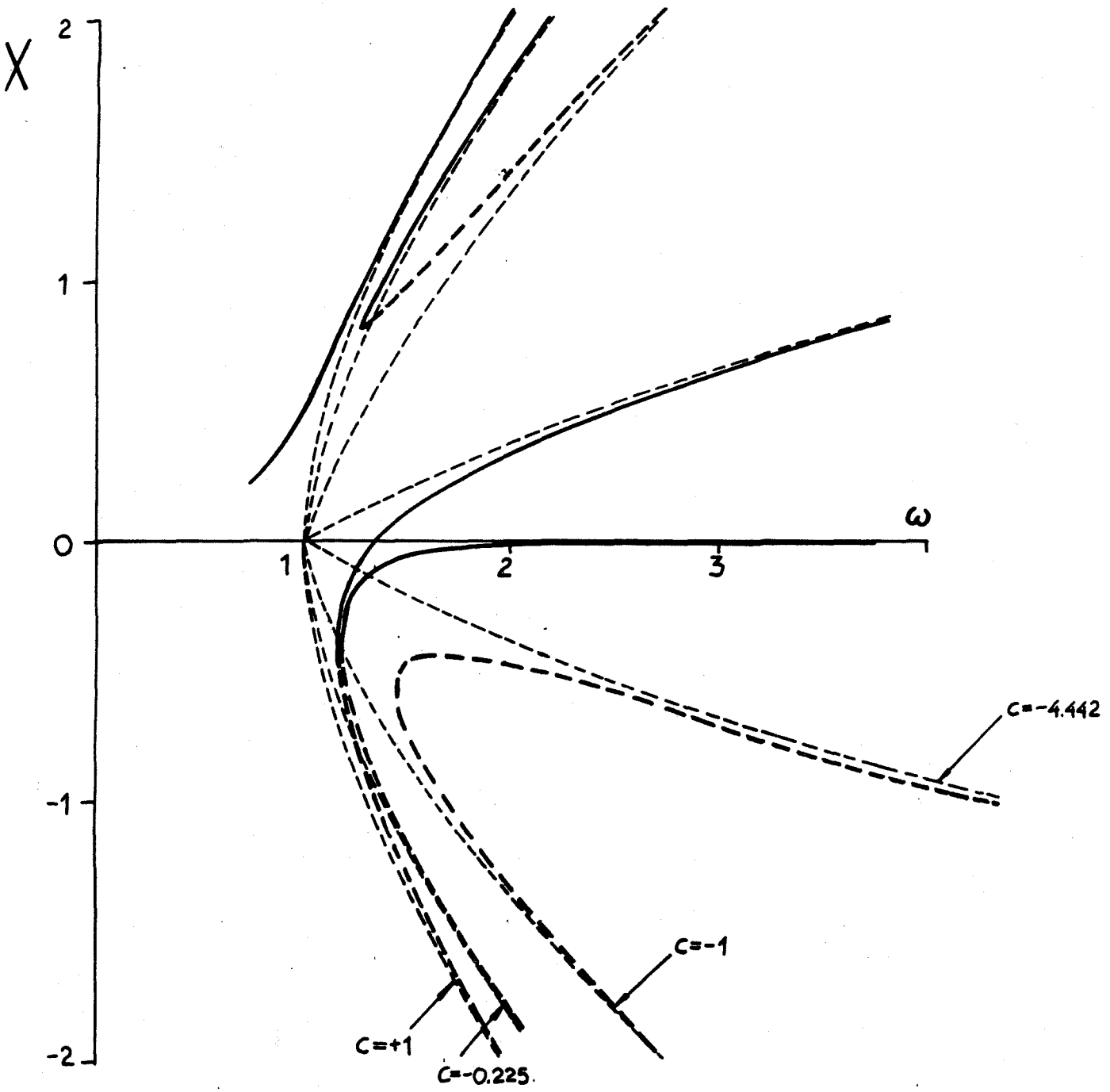

Figure 25. Response curves for the symmetric system for $r=0.15 < 1/4$. Stable solutions _____. Unstable solutions ----------

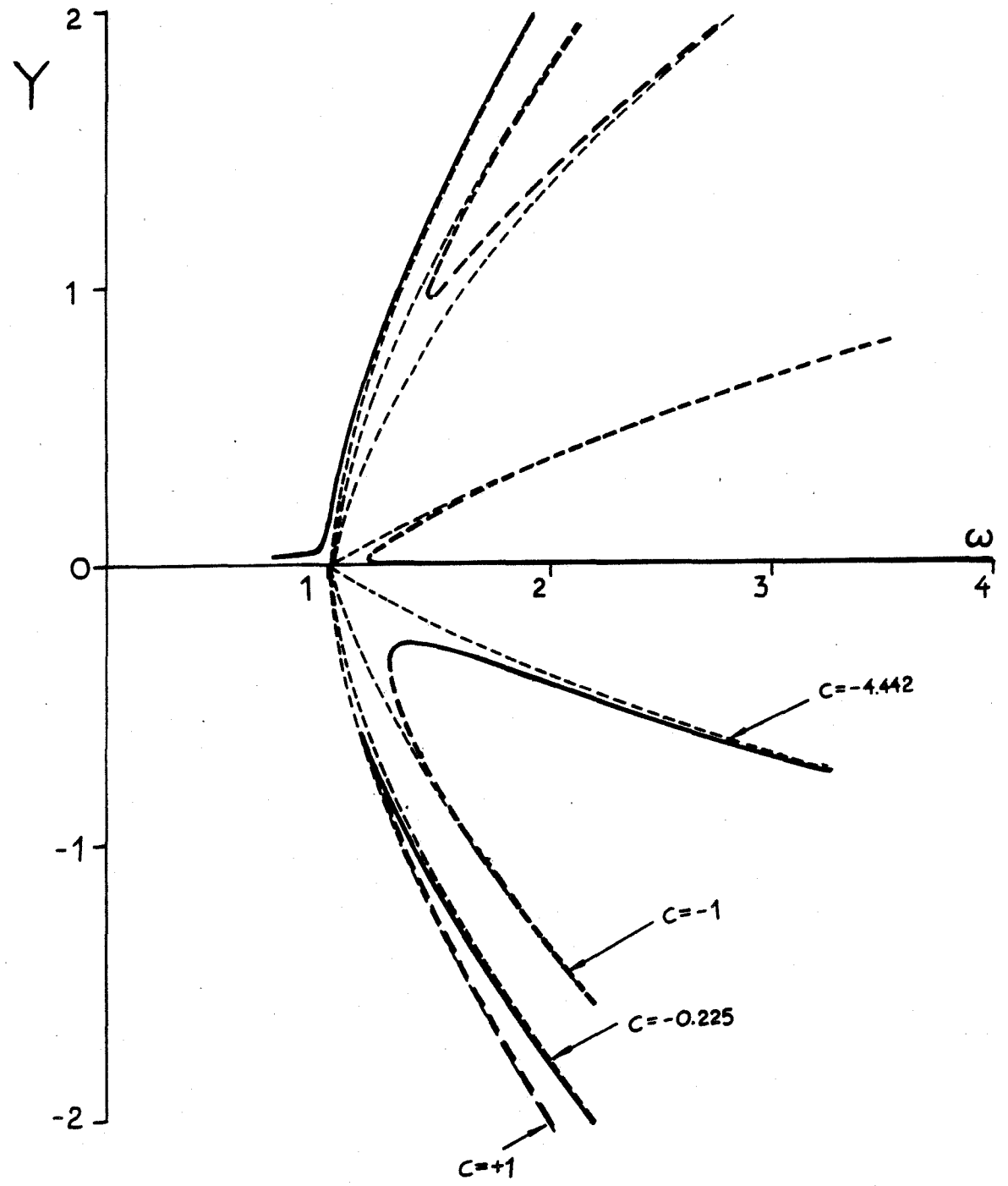
Y
2
1
0
-1
-2
ω
1
2
3
4
C=-4.442
C=-1
C=-0.225
C=+1

As far as the displacements of the system are concerned, we have three distinct cases depending on the ratio of the frequency of oscillation ω and the square root of the linear term of the end springs $f_{11}^{1/2}$.

(a) Hardening Duffing Response: If $\omega/f_{11}^{1/2} > 1$, then we have that $\mu_3 > 0$ and the displacement $x(t)$ is given by the fisrt of equations (4.16) and $y = cx$. The forcing necessary for the steady state is then

$$p(t) = \left(\frac{P}{X}\right)^3 x^3(t) \tag{4.19}$$

(b) Softening Duffing Response: If $\omega/f_{11}^{1/2} < 1$, then we have that $-f_{11}/X^2 < \mu_3 < 0$ and we have to use the second of equations (4.16) to compute $x(t)$. Note that,

$$\lim_{\mu_3 \to -f_{11}/X^2} k_2 = 1 \Rightarrow \lim_{\mu_3 \to -f_{11}/X^2} K(k_2) = \infty \tag{4.20}$$

and hence, from equations (4.17), we have

$$\lim_{\omega \to 0} \mu_3 = -f_{11}/X^2 \tag{4.21}$$

We therefore conclude that no unbounded motions can be physically realised (with $\mu_3 < -f_{11}/X^2$), since this would imply that $\omega < 0$ and thus a negative frequency of oscillation.

(c) Harmonic case: Finally we have the special case $\omega = f_{11}^{1/2}$ and in this case we obtain $\mu_3 = 0$ and the system responds harmonically:

$$x(t) = X \cos(f_{11}^{1/2} t)$$

$$y(t) = c\,x(t) \tag{4.22}$$

where c and X can be computed from equations (4.15), as

$$c = \left[1 + \left(f_{13}/f_{23}\right)^{1/3}\right]^{-1} \quad , \quad X = \frac{P}{(1+c)\, f_{13}^{1/3}} \tag{4.23}$$

In this case, the necessary forcing for a harmonic steady state, is:

$$p(t)= P^3 \cos^3(f_{11}^{1/2} t) \qquad (4.24)$$

Note that the above harmonic solution is exact, in the sense that no approximation concering the smallness of the nonlinearities or the amplitude was made. However, as we can see from the above solution, this special steady state is only valid for a particular value of the frequency ω , namely $\omega= f_{11}^{1/2}$.

Concluding the analysis of this section, it must be stated that response curves similar to those of figure 24 are reported in [2,16] for the symmetric "Homogeneous" system. However in these references, $f_{11}=0$, and thus the two backbone curves start from the origin of the axes and no harmonic steady state is possible.

4.2. SYSTEMS WITH NO ADDITIONAL NORMAL MODES

4.2.1. EXACT STEADY STATES

The examination of the steady state motion of this class of systems has to be carried on a case to case basis and we will demonstrate the methodology with a specific application. Consider the same symmetric system with cubic nonlinearities studied in the previous section, but now with a linear term present in the coupling spring f_2 :

$$\begin{aligned} f_1(u)&= f_{11}u+ f_{13}u^3 \\ f_2(u)&= f_{21}u+ f_{23}u^3 \\ f_3(u)&= f_1(u) \end{aligned} \qquad (4.25)$$

It was shown in [1], that with a linear term present in the coupling spring, no additional normal modes of free oscillation are possible and thus the system can freely oscillate only in the symmetric or anti-symmetric modes $(c=\pm 1)$.

Consider now a forcing function related to the steady state displacement by:

$$p(t)= \tilde{P}(x(t))= \left(\frac{P_1}{X}\right)x(t)+ \left(\frac{P_3}{X^3}\right)x^3(t) \qquad (4.26)$$

To show why the forcing must have the form (4.26), it is necessary to consider the "Balancing Diagrams" of the linear and nonlinear terms for the system under investigation. To find these diagrams, we use the modal relation (to be satisfied at the steady state) $y=cx$ and equation (4.26), to get the following differential equations of motion:

$$\ddot{X}+X\left[f_{11}+f_{21}(1-c)-\frac{P_1}{X}\right]+X^3\left[f_{13}+f_{23}(1-c)^3-\frac{P_3}{X^3}\right]=0$$

$$\ddot{X}+X\left[-f_{21}\left(\frac{1-c}{c}\right)+f_{11}\right]+X^3\left[f_{13}c^2-f_{23}\frac{(1-c)^3}{c}\right]=0 \qquad (4.27)$$

where the usual set of initial conditions (4.8) is assumed, with the addition $Y=cX$. Again, to obtain a steady motion, both equations (4.27) must yield the same wave form for $x(t)$ and hence we require that:

$$f_{11}+f_{21}(1-c)-\frac{P_1}{X}=-f_{21}\left(\frac{1-c}{c}\right)+f_{11}=\lambda^2 \qquad (4.28)$$

$$f_{13}+f_{23}(1-c)^3-\frac{P_3}{X^3}=f_{13}c^2-f_{23}\frac{(1-c)^3}{c}=\mu^2$$

We imposed the additional restriction that quantities (4.28) be positive, in order to investigate the "Hardening Duffing" responce of the system ($\mu^2>0$). If we want to investigate any possible "Softening Duffing" responses, we just have to substitute μ^2 in the second equation (4.28), with $-\mu^2$. Then we must check that the resulting frequency of oscillation ω is a positive quantity (that the motions are physsically realisable).

In figures 26 and 27, we schematically present the solution for c for each of the two equations (4.28), as functions of the ratios f_{21}/f_{11} and f_{23}/f_{13} respectivelly. The diagrams 26(a) and 27(b) corresponding to $P_1=P_3=0$, are used to find the values of the modal parameter c for free vibration motions. Since both of the aforementioned diagrams need to be satisfied, we see that for free oscillations, c can have only the values ± 1 , corresponding to the symmetric and antisymmetric modes respectivelly (in the previous section, no such restriction holds, since $f_{21}=0$ and no linear Balancing Diagram exists). When the forcing is applied, the Balancing Diagrams are distorted

and the steady state values of c must satisfy both of them simultaneously. Hence, in order for a steady state to occur, we must perturb both Balancing diagrams and this is achieved when the forcing is of the form (4.26), i.e. contains a linear and a cubic term in the displacement $x(t)$. We therefore conclude, that when a system has more than one Balancing Diagrams of free oscillation, the necessary excitation for steady state motions should be such, as to perturb all of the Diagrams simultaneously. Thus, the forcing necessary for the steady state must be expressed in a series form and the number of terms in the series must be equal to the number of Balancing Diagrams of free oscillation of the system. The term of the series representing a particular Balancing Diagram, must be proportional to the displacement raised to a power equal to that of the nonlinearity of the Balancing Diagram.

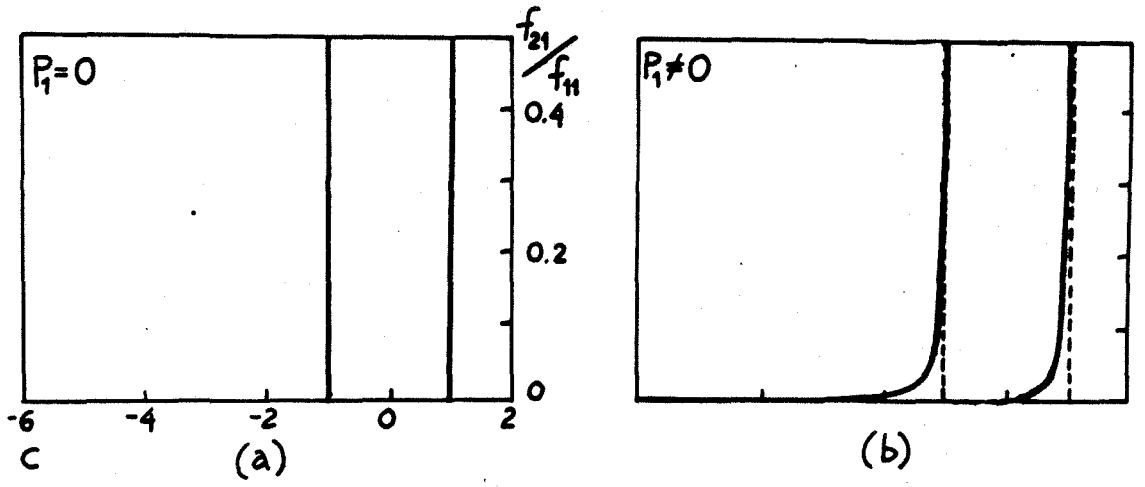

Figure 26. Balancing Diagrams of Linear terms
(a) Unforced (b) Forced

Assuming now that equations (4.28) hold, we derive the response of the system as follows:

$$x(t)=X\,cn(qt/k)\ ,\ y(t)=cx(t) \tag{4.29}$$

where

$$q^2=\lambda^2+\mu^2X^2\ ,\ k^2=\mu^2X^2/2q^2 \tag{4.30}$$

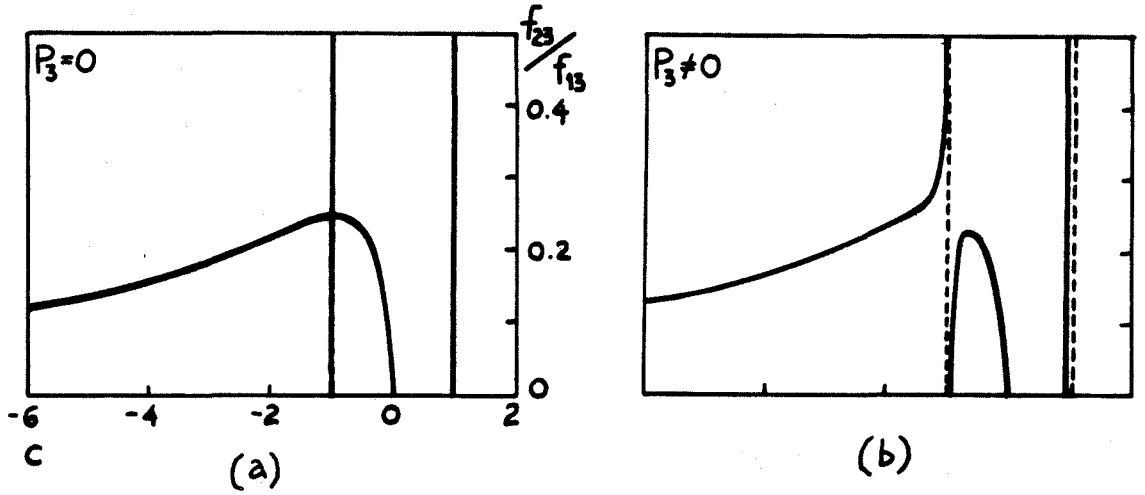

Figure 27. Balancing Diagrams of Cubic terms
(a) Unforced (b) Forced

and

$$c = f_{21}/(f_{11}+f_{21}-\lambda^2)$$
$$P_1/X = (f_{11}-\lambda^2)(f_{11}+2f_{21}-\lambda^2)/(f_{11}+f_{21}-\lambda^2)$$
$$\mu^2 = (f_{13}f_{21}^3 - f_{23}(f_{11}-\lambda^2)^3)/f_{21}(f_{11}+f_{21}-\lambda^2)^2 \qquad (4.31)$$
$$P_3/X^3 = f_{31}+f_{32}(1-c)^3-\mu^2$$

We see that all quantities in (4.31) are expressed in terms of the quantity λ^2 and this variable can be related to the frequency of oscillation ω, by:

$$\omega = \frac{\pi[\lambda^2+\mu(\lambda)^2X^2]^{1/2}}{2K(k(\lambda))} \qquad (4.32)$$

where $K(\cdot)$ is the complete elliptic integral of the first kind and k is the elliptic modulus. Expression (4.32) relates the amplitude of oscillation X to the frequency ω and therefore gives the response curves of the system at the steady state. The necessary forcing can be found from (4.26), by substituting the expression for $x(t)$ (from 4.29)):

$$p(t) = P_1 cn(qt/k) + P_3 cn^3(qt/k) \qquad (4.33)$$

By setting $P_1 = P_3 = 0$, eq uations (4.28) and (4.31) give the free vibration solution for the class of systems under consideration (symmetric and containing a linear coupling term). As discussed previously, only two motions are possible:

$$c=+1\,,\ \lambda^2 = f_{11}\,,\ \mu^2 = f_{13} \qquad \text{(Symmetric Mode)}$$

$$c=-1\,,\ \lambda^2 = f_{11}+2f_{21}\,,\ \mu^2 = f_{13}+8f_{23} \qquad \text{(Antisymmetric Mode)}$$

Using the above results for λ^2 and μ^2 , we can compute the backbone response curves from expression (4.32) and it can be seen that as long as the linear term of the coupling spring is nonzero, only two backbone curves can exist, since the only real roots for c are $+1$ or -1 . It can be stated therefore that, in contrast to what was found for the system with additional normal modes (section 4.1), the topological portrait of the response curves of the class of systems under consideration, does not change with a change in the structural parameters of the system, since no additional backbone curves can be generated.

Consider now the case $P_1, P_3 \neq 0$. By examining relations (4.31), it can be easily seen that if either one of P_1 or P_3 is taken as constant, the other must be made dependent on the frequency of oscillation ω . This fact leads to some difficulty in defining an acceptable constant "Forcing Amplitude" for the steady state and to solve this problem we follow the perturbation method of Hsu [18], who studied the exact forced steady state of the Single Degree of freedom system. Even though solution (4.29-4.32) is difficult to interprete physically, nevertheless it is an exact steady state solution and as we will show in the next section it leads to the well known approximate harmonic steady state, if we let the nonlineartities to become small (of perturbation order). As a last remark we note that the forcing form (4.33) is the only one leading to a steady state motion. However as shown in [1], if we take the excitation to be proportional to the displacement we obtain a "Pseudo - steady state" motion, namely a periodic motion only valid for a particular frequency ω .

4.2.2. PERTURBATION ANALYSIS - APPROXIMATE STEADY STATE MOTIONS

The analysis presented in this section, is similar to that carried in [18], where the exact steady state of the Single

Degree of freedom system excited by the forcing (4.26), was examined. Assume to this end that the quantities $f_{i3}X^2$ are small:

$$0 < f_{i3}X^2 \ll 1 \ , \quad i=1,2 \tag{4.34}$$

This either implies that the nonlinearities f_{i3} are small or that the amplitudes of motion are small. From expressions (4.31) and assuming that $f_{i1}=O(1)$, $i=1,2$, we conclude that the elliptic modulus k^2 is also small, namely of perturbation order. Expanding now the elliptic cosine and its cube in (4.33) (using the expansions listed in the Appendix), and retaining only terms of order k^2, we obtain:

$$p(t)=P_1(a_1\cos\omega t+a_3\cos 3\omega t)+P_3(b_1\cos\omega t+b_3\cos 3\omega t)+O(k^4) \tag{4.35}$$

were the coefficients a_i and b_i were also expanded in k^2 :

$$\begin{aligned} a_1&=1-\frac{k^2}{16}+\dots \\ a_3&=\frac{k^2}{16}+\dots \\ b_1&=\frac{3}{4}-\frac{35k^2}{64}+\dots \\ b_3&=\frac{1}{4}+\frac{6k^2}{128}+\dots \end{aligned} \tag{4.36}$$

Eliminating now the quantity λ^2 from expressions (4.30–4.31) and rearranging terms, we find the following forms for the forces in terms of the three parameters c, k and q :

$$\begin{aligned} \frac{P_3}{X^3}&=f_{13}+f_{23}(1-c)^3-\frac{2k^2q^2}{X^2} \\ \frac{P_1}{X}&=(2k^2-1)q^2+f_{11}+f_{21}(1-c) \end{aligned} \tag{4.37}$$

Finally substituting (4.37) into (4.36), we obtain the following expression for the force acting on the system correct to $O(k^2)$:

$$\begin{aligned} p(t)=&\left\{\left[(2k^2-1)q^2+f_{11}+f_{21}(1-c)\right]Xa_1+\left[f_{13}+f_{23}(1-c)^3-\frac{2k^2q^2}{X^2}\right]X^3b_1\right\}\cos\omega t+ \\ &+\left\{\left[(2k^2-1)q^2+f_{11}+f_{21}(1-c)\right]Xa_3+\left[f_{13}+f_{23}(1-c)^3-\frac{2k^2q^2}{X^2}\right]X^3b_3\right\}\cos 3\omega t+ \\ &+O(k^4) \end{aligned} \tag{4.38}$$

A similar expansion in terms of k^2 can be carried out with the response $x(t)$ given by (4.29):

$$x(t)= a_1 X\cos\omega t + a_3 X\cos 3\omega t + \ldots = X\cos\omega t + O(k^2) \qquad (4.39)$$

We see that for k^2 sufficiently small, we obtain a dominant harmonic term with frequency ω in the response and small additional terms containing higher harmonics.

Observing now equations (4.38) and (4.39), we conclude that if we set

$$\left[(2k^2-1)q^2 + f_{11} + f_{21}(1-c)\right] X a_1 + \left[f_{13} + f_{23}(1-c)^3 - \frac{2k^2q^2}{X^2}\right] X^3 b_1 = P_o$$

$$\left[(2k^2-1)q^2 + f_{11} + f_{21}(1-c)\right] X a_3 + \left[f_{13} + f_{23}(1-c)^3 - \frac{2k^2q^2}{X^2}\right] X^3 b_3 = 0 \qquad (4.40)$$

we ensure that, with an accuracy up to $O(k^2)$, the system is excited with a harmonic force $P_o\cos\omega t$ and the response is also harmonic and of the same frequency with that of the excitation. In the above expressions, P_o is the constant amplitude of the harmonic excitation. Thus we see that by letting the nonlinearities and/or the displacements to become small, the exact steady state solution (4.29-4.33) degenerates to an approximate harmonic steady state solution. To study this approximate harmonic motion, we have to eliminate the variables q and c from equation (4.40) and this is achieved as follows:

By expanding the complete elliptic integral $K(k)$ in terms of its modulus and using the definition of q from (4.30), equation (4.32) becomes:

$$q^2 = \left(1 + \frac{k^2}{2}\right)\omega^2 + O(k^4) \qquad (4.41)$$

We then use equations (4.30) and (4.31) to relate c and q with the following expression:

$$q^2 = \lambda^2 + \mu^2 X^2 = -f_{21}\frac{1-c}{c} + f_{11} + \left[f_{31}c^2 - f_{32}\frac{(1-c)^3}{c}\right] X^2 \qquad (4.42)$$

Finally combining (4.40-4.42), we get the following set of equations which describes the approximate harmonic steady state correct to $O(k^2)$:

$$f_{11}+f_{21}(1-c)-\omega^2-\frac{P_o}{X}+\left[f_{13}+f_{23}(1-c)^3\right]X^2\left\{\frac{7\omega^2-f_{11}-f_{21}(1-c)}{9\omega^2-f_{11}-f_{21}(1-c)}\right\}=0$$

$$c=f_{21}/(f_{11}+f_{21}-\omega^2)$$

$$k^2=\frac{4\left[f_{13}+f_{23}(1-c)^3\right]X^2}{9\omega^2-\left[f_{11}+f_{21}(1-c)\right]} \qquad (4.43)$$

By eliminating c from the first two equations we obtain the Amplitude - Frequency response curves for a fixed value of the forcing P_o. It must be pointed out that the above approximate steady state motion is valid for all frequencies except for those in the neighbourhood of $\omega\simeq(f_{11}+f_{21}(1-c))/9$, since for these frequencies the denominator of the last of equations (4.43) becomes a small quantity and then k^2 is not any more of perturbation order. Also note that from the first of equations (4.43) we have that (note that $c=O(1)$):

$$f_{11}+f_{21}(1-c)-\omega^2-\frac{P_o}{X}=O(k^2) \qquad (4.44)$$

and this implies that soluction (4.43) represents a small perturbation of the linear harmonic steady state.

In figure 28, we presend the approximate steady state responses for a system with $f_{11}=1.0$, $f_{21}=4.0$, $f_{13}=0.07$, $f_{23}=0.1$, and $P_o=0.05$. The stability question concerning these solutions is addressed elsewhere [20,21] and it can be shown that two solution branches are orbitally unstable.

Summarising, we demonstrated that the exact steady state solution (4.29)-(4.33) valid for the strongly nonlinear system, is a generalisation of the approximate harmonic steady state solution, since it degenerates to this later motion when the nonlinearities and/or the displacements become small. However, as pointed out by Hsu [18], an approxiamte Subharmonic motion can also result. To show this, consider again equation (4.38), but instead of imposing conditions (4.40), require that:

$$\left[(2k^2-1)q^2+f_{11}+f_{21}(1-c)\right]Xa_1+\left[f_{13}+f_{23}(1-c)^3-\frac{2k^2q^2}{X^2}\right]X^3b_1=0$$

$$\left[(2k^2-1)q^2+f_{11}+f_{21}(1-c)\right]Xa_3+\left[f_{13}+f_{23}(1-c)^3-2k^2q^2/X^2\right]X^3b_3=P_o \qquad (4.45)$$

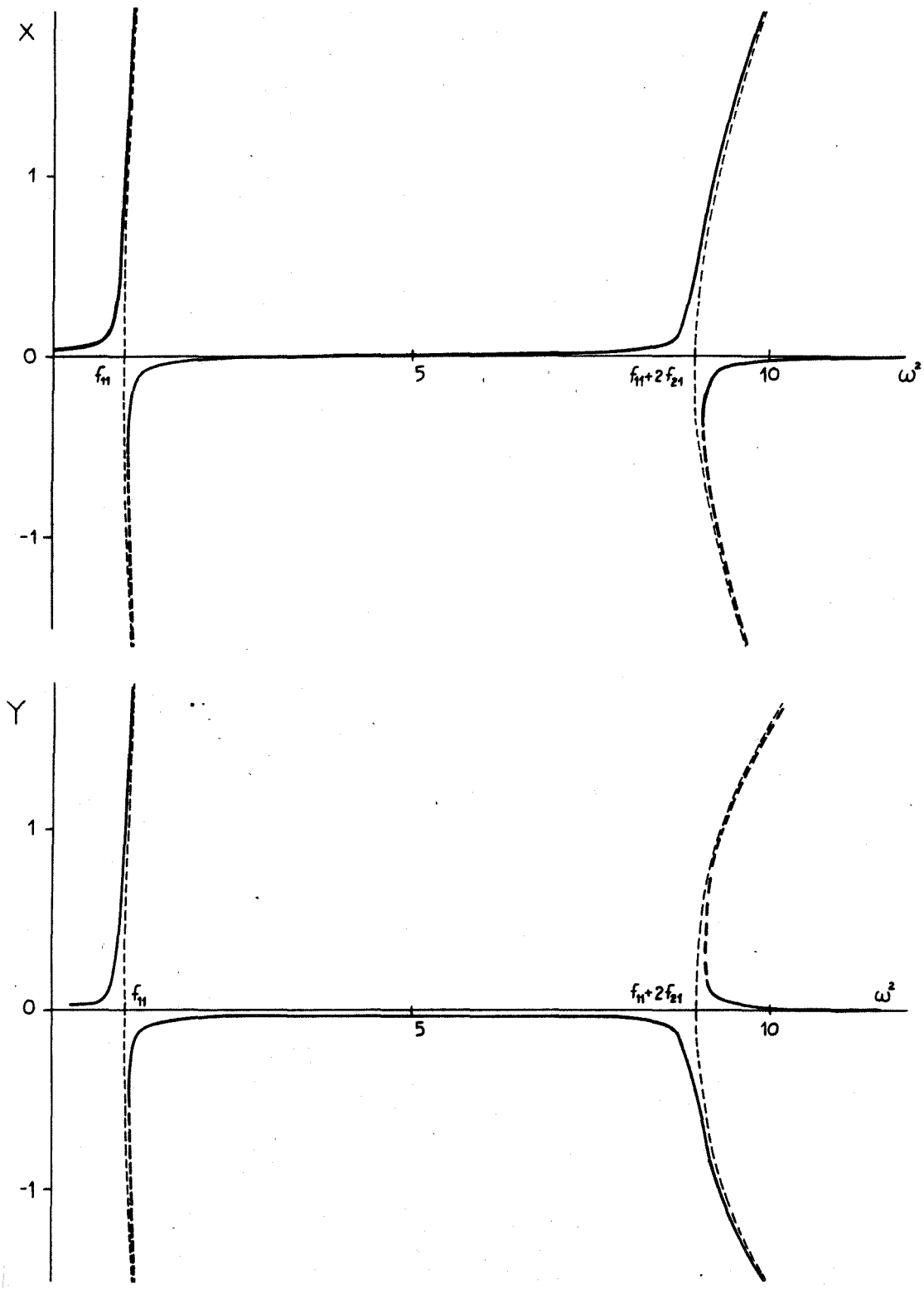

Figure 28. Approximate Harmonic Steady State Responses.
Stable _____, Unstable ----------

The result is that the forcing applied to the system is approximatelly harmonic, with frequency three times that of the frequency of the harmonic response.

$$p(t) = P_0 \cos 3\omega t + O(k^4)$$

$$x(t) = X \cos \omega t + O(k^2) \qquad (4.46)$$

This is clearly the approximate subharmonic phenomenon.

4.3. DISCUSSION

In this section the exact steady states of symmetric, undamped, strongly nonlinear systems were examined. Although we have considered systems of only two degrees of freedom, the methodology presented can be easily extended to systems with arbitrarily many DOF, by considering suitable forcing functions and introducting linear relations between the coordinates of the system. An uncoupling of the differential equations of motion can then follow, in a similar way to that presented in this work.

It was shown that an important problem in studying the exact steady states of strongly nonlinear systems, is how to chose the right from of the exciting force that produces these motions. This problem was solved in this work by selecting the excitation in such a way as to transform the forced motion to an equivalent free oscillation. We achieved this, by expressing the excitation as a function of the steady state displacement and by assuming that at the steady state the displacements of the system are linearly dependent. We then used a matching procedure to uncouple the equation of motion of the system and we obtained the response of the system by quadratures. We examined two categories of systems. In the first case, the system possesed additional modes of free oscillation and the force was taken to be proportional to the displacement raised to a power equal to that of the nonlinearity. In the second case, the system had only two modes of free vibration and the forcing contained a term linear in the displacement and a term with the displacement raised to a power equal to that of the nonlinearity. The steady

motions of such systems have to be examined on a case to case basis and the forcing must be related to the displacement in such a way, as to ensure that every Balancing Diagram of linear and nonlinear terms is excited.

Explicit expressions for the Amplitude-Frequency response curves were derived and their topology was examined by considering the number of backbone curves of free oscillaton present in the system. It was shown that if a nonlinear system posseses additional normal modes, the topological portrait of its response curves may change, if a certain structural parameter is changed. For systems with no additional normal modes of free oscillation, this does not hold and the form of the response curves remains analtered with changes of their structural parameters.

Specific applications were given for systems with cubic nonlinearities. For a system with a linear term in the coupling spring, a difficulty was encountered in finding a constant modulus for the acting force, but nevertheless, by using Hsu's perturbation methodology, we showed that the exact steady state found here is a generalisation of the well known approximate harmonic response of the weakly nonlinear system, acted by a harmonic forcing.

Finally, we should state that although we considered here only symmetric systems, the same methodology applies to the nonsymmetric system shown in section 1. These systems were shown to possessnormal modes of free oscillation and the principle of the exact steady state can also be applied for that class of systems.

5. NONLINEARLY RELATED (NONSIMILAR) MODES

Until now we have examined similar normal modes of free oscillation, i.e. motions where the coordinates of the system are linearly related for all times. As pointed out by Rosenberg [2], for nonlinear systems, it is possible the existense of nonsimilar normal modes, in which the coordinates of the system are related by nonlinear functions for all times.

Generally no exact method exists for analysing these modes and only approxiamte analyses are reported in the literature [22-25]. In this last section, we will follow a different formulation of the problem than the one followed in the aforementioned literature. We do this, because we want to extend the matching procedure developed for the study of similar normal modes, to the study of nonsimilar ones. Hence the general methodology will be,

to assume a general nonlinear relation between the coordinates of the system and then attempt to uncouple the equations of motion by suitably matching coefficients of respective powers of the displacement $x(t)$. We discuss the limitations of the method, which are of the same nature with the ones encountered in existing analyses and we close the section by applying the method to a specific example.

5.1. ANALYSIS

Consider the two Degree of Freedom system of figure 1. Necessary conditions for the existense of similar normal modes in this system were derived in [1] and in this section we intend to examine a system for which these conditions are violated. Thus assume that the stiffnesses of the system have the form:

$$\begin{aligned} f_1(u) &= u+u^3 \\ f_2(u) &= K_1 u + K_3 u^3 \\ f_3(u) &= u+(1+\varepsilon)u^3 \end{aligned} \tag{5.1}$$

The differential equations of motion are:

$$\begin{aligned} &\ddot{x}+x+x^3+K_1(x-y)+K_3(x-y)^3=0 \\ &\ddot{y}+y+(1+\varepsilon)y^3+K_1(y-x)+K_3(y-x)^3=0 \end{aligned} \tag{5.2}$$

and the initial conditions $x(0)=X$, $\dot{x}(0)=0$, $y(0)=Y$, $\dot{y}(0)=0$ are assumed. To show that no similar normal modes are possible for this system, substitude the condition $y=cx$ in (5.2), to obtain:

$$\begin{aligned} &\ddot{x}+x[1+K_1(1-c)]+x^3[1+K_3(1-c)^3]=0 \\ &\ddot{x}+x\left[1+K_1\frac{(c-1)}{c}\right]+x^3\left[(1+\varepsilon)c^2+K_3\frac{(c-1)^3}{c}\right]=0 \end{aligned} \tag{5.3}$$

By matching the linear and cubic terms in the above set of equations, we obtain the Balancing Diagram of figure 29. Clearly there is no real value of c satisfying both Balancing Diagrams and hence we conclude that no similar normal modes exist for this system, if $\varepsilon \neq 0$. On the other hand, with $\varepsilon = 0$, we recover the symmetric system, which as we know posses two similar normal modes $c=\pm 1$. Thus the system described by the equations of motion (5.2), can be regarded as a "perturbed" system, close (in some sense) to an "unperturbed" system which posseses similar normal modes.

So, returning to the differential equations of motion (5.2), we seek a nonlinear relation

$$y = f(x) \tag{5.4}$$

that is to be satisfied for every instant of time t .
Differentiating (5.4) we obtain

$$\dot{y} = f'(x)\dot{x} \ , \ \ddot{y} = f''(x)(\dot{x})^2 + f'(x)\ddot{x} \tag{5.5}$$

where $(\,)' \equiv d/dx$, $(\dot{}) \equiv d/dt$. Substituting now expressions (5.4) and (5.5) into the equations of motion (5.2), we have:

$$\begin{aligned} &\ddot{x} + x + x^3 + K_1 x - K_1 f(x) + K_3 (x - f(x))^3 = 0 \\ &f''(x)(\dot{x})^2 + f'(x)\ddot{x} + f(x) + (1+\varepsilon) f^3(x) + K_1 f(x) - K_1 x + K_3 (f(x) - x)^3 = 0 \end{aligned} \tag{5.6}$$

Consider now the set of differential equations (5.6). The quantity $(\dot{x})^2$ in the second equation can be expressed by a direct integration of the fisrt equation:

$$(\dot{x})^2 = -\int_X^x \left\{ \xi(1+K_1) + \xi^3 - K_1 f(\xi) + K_3 (\xi - f(\xi))^3 \right\} d\xi \tag{5.7}$$

where the usual initial conditions $x(0) = X$, $\dot{x}(0) = 0$, $y(0) = Y = f(X)$, $\dot{y}(0) = 0$ are assumed. Substituting relation (5.7) into the second of equations (5.6) and rearranging terms, we obtain the following final set of differential equations:

$$\begin{aligned} &\ddot{x} + x + x^3 + K_1 x - K_1 f(x) + K_3 (x - f(x))^3 = 0 \\ &\ddot{x} f'(x) - f''(x) \int_X^x \left\{ \xi(1+K_1) + \xi^3 - K_1 f(\xi) + K_3 (\xi - f(\xi))^3 \right\} d\xi + \\ &+ f(x) + (1+\varepsilon) f^3(x) + K_1 f(x) - K_1 x + K_3 (f(x) - x)^3 = 0 \end{aligned} \tag{5.8}$$

We see that both are differential equations of x and that both have x differentiated to the second order in t .

We now list certain properties of nonsimilar normal modes, which introduce restrictions in the form of the functional relation $y=f(x)$.

(a) The nonsimilar normal mode, is a periodic motion passing through the origin of the configuration space. So, it must be satisfied that $f(0)=0$.

(b) Since the potential energy of the system was assumed to be symmetric with respect to the origin of the configuration space (see section 1), the normal modes must satisfy [2]: $y(-x)=-y(x) \Rightarrow f(-x)=-f(x)$.

(c) Finally the nonsimilar Normal Modes must intersect orthogonally the "Bounding Curve Γ " [2], denoting the equipotential curve in the configuaration plane, corresponding to the maximum amplitudes for the system.

From (a), (b), and (c) we conclude that the nonsimilar normal mode must have the appearance of figure 30 and that it can be represented by the following expansion in odd powers of x :

$$y=f(x)=a_1x+a_3x^3+a_5x^5+\dots \tag{5.9}$$

Assuming that $f(x)$ is related to x by the series expression (5.9), the set of differential equations (5.8), becomes:

$$\ddot{x}+x\ [1+K_1-K_1a_1]+x^3[1-a_3K_3+K_3(1-a_1)^3]+\dots=0$$

$$\ddot{x}+x\left\{\frac{3a_3x^2[1+K_1(1-a_1)]}{a_1}+\frac{3}{2}\frac{a_3}{a_1}\left[1-K_1a_3+K_3(1-a_1)^3\right]x^4+1+K_1-\frac{K_1}{a_1}\right\}+$$

$$+x^3\left\{-\frac{3a_3}{a_1}[1+K_1(1-a_1)]+10\frac{a_5x^2}{a_1}[1+K_1(1-a_1)]+\frac{a_3}{a_1}+\right. \tag{5.10}$$

$$+(1+\varepsilon)a_1^2+K_1\frac{a_3}{a_1}+K_3\frac{(a_1-1)^3}{a_1}-\frac{9a_3^2x^2}{a_1^2}[1+K_1(1-a_1)]-$$

$$\left.-\frac{9a_3^2}{2a_1^2}[1-K_1a_3+K_3(1-a_1)^3]x^4-\frac{3a_3}{a_1}-\frac{3K_1a_3}{a_1}+\frac{3K_1a_3}{a_1^2}\right\}+\dots=0$$

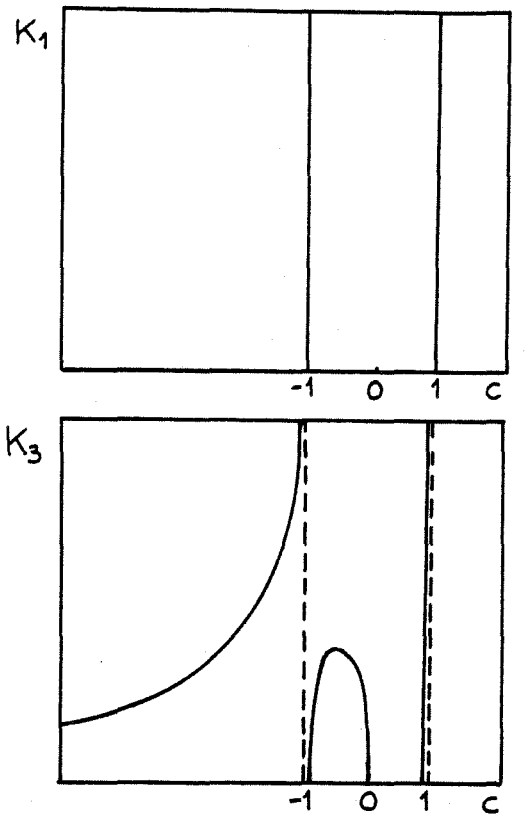

Figure 29. Balancing Diagrams of the system with nonsimilar Normal Modes.

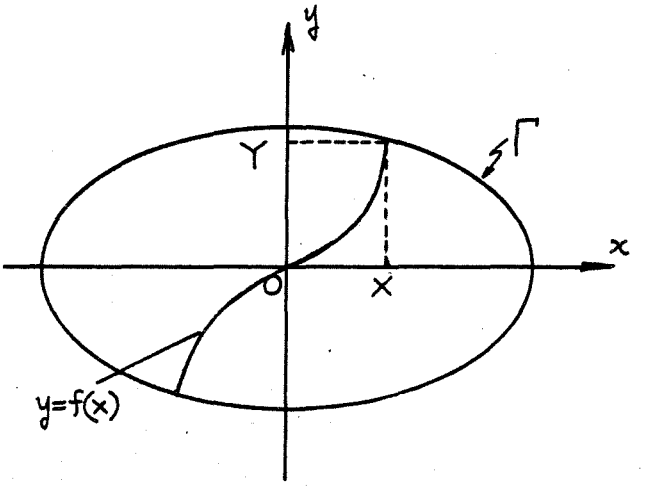

Figure 30. Nonsimilar Normal Modes.

where the terms omitted in (5.10) contain powers of x, greater than three. Matching coefficinets of respective powers of X, in a similar way as before, we obtain the following balancing equation.

Terms in X : $$-K_1 a_1^2 = 3a_3[1+K_1(1-a_1)]X^2 + \frac{3}{2}a_3[1-K_1 a_3 + K_3(1-a_1)^3]X^4 - K_1$$

Terms in X^3 : $$1-a_3K_3+K_3(1-a_1)^3 = -\frac{3a_3}{a_1}[1+K_1(1-a_1)] + \frac{10a_5X^2}{a_1}[1+K_1(1-a_1)] +$$
$$+\frac{a_3}{a_1} + (1+\varepsilon)a_1^2 + K_1\frac{a_3}{a_1} + K_3\frac{(a_1-1)^3}{a_1} - \frac{9a_3^2X^2}{a_1^2}[1+K_1(1-a_1)] -$$
$$-\frac{9a_3^2}{2a_1^2}[1-K_1a_3+K_3(1-a_1)^3]X^4 - \frac{3a_3}{a_1} - \frac{3K_1a_3}{a_1} + \frac{3a_3K_1}{a_1^2} \qquad (5.11)$$

From the first of equations (5.11), we obtain a relation between a_1 and a_3, and from the second, a relation between a_1, a_3, and a_5. Each additional balancing equation (matching coefficinets of $X^5, X^7, \ldots$) will introduce additional unknowns ($a_7, a_9, \ldots$) and we see that in order to determine the constants a_i, an additional equation is needed.

To find this additional condition, eliminate $\ddot{x}$ from equations (5.8) and get the following functional equation for $f(x)$:

$$-f''(x)\left\{\frac{(x^2-X^2)}{2}(1+K_1) + \frac{(x^4-X^4)}{4} + \int_X^x \left\{K_3(\xi - f(\xi))^3 - K_1 f(\xi)\right\} d\xi\right\} -$$
$$-f'(x)\left\{x+x^3+K_1x-f(x)K_1+K_3(x-f(x))^3\right\} + f(x)+(1+\varepsilon)f^3(x)+K_1f(x) - \qquad (5.12)$$
$$-K_1x+K_3(f(x)-x)^3 = 0$$

The function $f(x)$ describing the normal mode oscillation must satisfy (5.12) and this equation is equivalent to the one formed in reference [23]:

$$2(h-V)y'' + (1+y'^2)(V_y - y'V_x) = 0 \qquad (5.13)$$

where $y=y(x)$ is the representantion of the nonsimilar normal mode the configuration plane, h is the total energy of the system and $V(x)$ is the potential energy.

We see that both equations (5.12) and (5.13) are singular at the Bounding Curve corresponding to $V=h$ and $x=X$, since the coefficients of the second derivatives of f and y vanish there. However, we can always find a series representation (5.9) which asymptotically approximates the solution every where in the open interval $(-X,X)$:

$$y=f(x)=a_1x+a_3x^3+a_5x^5+\dots \quad , -X<x<X \tag{5.14}$$

But we have the requirement that the nonsimilar normal modes must interest the "Bounding curve Γ " and thus we must analytically continue the solution (5.14) until it intersects the boundary Curve. So, to guarantee that the mode intersects the curve Γ at $(x,y)=(X,Y)$, we must require that:

$$-f'(X)\left\{X+X^3+K_1X-f(X)K_1+K_3\left(X-f(X)\right)^3\right\}+f(X)+$$

$$+(1+\varepsilon)f(X)^3+K_1f(X)-K_1X+K_3\left(f(X)-X\right)^3=0 \tag{5.15}$$

or equivalently, for representation (5.13):

$$\left(V_y-y'V_x\right)_{V=h}=0 \tag{5.16}$$

Equations (5.15) and (5.16) were obtained from equations (5.12) and (5.13) respectively, by setting $x=X$ and $V=h$. As mentioned previously, they satisfy the condition that the analytic continuations of the series expressions for the modes, intersect the Bounding curve Γ (see figure 30).

Substituting the series expression (5.14) into (5.15), we obtain

$$K_3X^2(1-a_1)^2(1-a_1^2)+K_1(1-a_1^2)+a_1X^2\left[(-1-\varepsilon)a_1^2+1\right]=$$

$$=4a_3a_1K_1X^2-2a_3(1+K_1)X^2+\dots \tag{5.17}$$

where we have omitted terms of $O(a_3 X^5)$ and terms containing a_i with $i \geq 5$. Equation (5.17) combined with equations (5.11), gives the solution for a_i and thus leads to the determination of the approximate representation (5.14) for the nonsimilar normal mode.

We will apply now the aforementioned method, to the examination of a weakly coupled system.

5.2. APPLICATION

We apply the ideas of the previous section to the coupled system of figure 31. In the notation of the previous section, we have

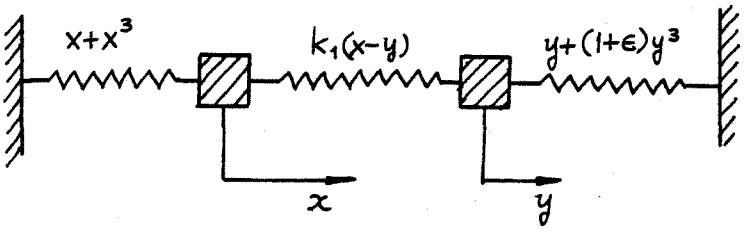

Figure 31. Weakly Coupled System

$K_3 = 0$, and we additionally require that $K_1 = O(\varepsilon)$, (note that ε is the structural perturbation that prohibits Similar Normal Modes). Assuming that ε is a small quantity, we conclude that the system of figure 31, is a weakly coupled system and we are interested in examining its nonsimilar normal modes.

In order to apply the aforementioned methodology we must assume small amplitudes of oscillation and thus we see that in our problem there exist two perturbation quantities: the structural parameter ε and the amplitude of oscillation X. To relate these two quantities assume that:

$$\varepsilon = O(X^2) \tag{5.18}$$

for $\epsilon=0$, the system has similar normal modes given by $a_1=\pm 1$ $\Rightarrow a_1^2=1$. So for sufficiently small, we assume that

$$a_1^2-1=O(\epsilon)=O(X^2) \tag{5.19}$$

and thus that the leading term of the representation (5.14) differs from the similar - mode value, only by $O(\epsilon)$ terms. Note that assumption (5.19) must be verified a posteriori, by the solution.

Using assumptions (5.18) and (5.19), the set of equations (5.11) and (5.17), lead to the following approximate solution (note that since we are interested only in , we have used only the first of equations (5.11):

$$\begin{aligned} 3a_3X^2&=(1-a_1^2)K_1+O(X^4)\\ 5(1-a_1^2)K_1&=3a_1X^2(a_1^2-1+\epsilon a_1^2)+O(X^6)\end{aligned} \tag{5.19}$$

Solution (5.19) requires that a_3 and $(1-a_1^2)$ are small quantities, of $O(X^2)$. The quantity a_1 is found from the second of equations (5.19) and subsequently a_3 is computed from the first. Then the approximate solution for the nonsimilar normal mode is given by (5.14) and it is only valid in the open interval $-X<x<X$. Note that if K_1 is not of perturbation order, then equations (5.19) cannot be balanced and the solution is not valid in this case. Thus, for each given problem, special cave should be taken, to solve equation (5.11) and (5.15), in a way that ensures balancing of terms of the same order of magnitude.

REFERENCES

1. Vakakis A.F. and Caughey T.K. 1988. Free and Forced Vibration of Certain Strongly Nonlinear Systems. Dynamics Laboratory Report DYNL - 88 - 1, California Institute of Technology, Pasadena, California.

2. Rosenberg R.M. 1966. On Nonlinear Vibration of Systems with Many Degrees of Freedom. Adv. Appl. Mech. 9, pp. 155-242.

3. Month L.A., Rand R. 1977. The Stability of Bifurcating Periodic Solutions in a Two - Degree - of - Freedom Nonlinear System. J. Appl. Mech., pp. 782-783.

4. Guggenheimer G., Holmes P. 1986. Nonlinear Oscillations, Dynamical Systems and Bifurcation of Vector Fields. Springer Verlang, New York.

5. Hayashi C. 1985. Nonlinear Oscillations in Physical Systems. Princeton Univ. Press, 1st Ed., Princeton, New Jersey.

6. Month L.A. 1979. On Approximate First Integrals of Hamiltonian Systems with an Application To Nonlinear Normal Modes in A Two Degree of Freedom Nonlinear Oscillator Ph. D. Thesis, Cornell Univ.

7. Month L.A. Rand R.H. 1980. An Application of the Poincaré Map to the Stability of Nonlinear Normal Modes. J. Appl. Mech., Vol. 47, pp. 645-651.

8. Lichtenberg A.J. Lieberman M.A. 1983. Regular and Stochastic Motion. Springer Verlag, New York.

9. Holmes P., Marsden J. 1982. Horseshoes in Perturbations of Hamiltonian systems with two Degrees of Freedom. Comm. Math. Physics 82, pp. 523.544.

10. Holmes P., Marsden J. 1982. Melnikov's method and Arnold diffusion for perturbations of integrable Hamiltonian systems. J. Math. Phys. 23(4), pp. 669-675.

11. Veerman P., Holmes P. 1985. The existense of Arbitrarily Many Distinct Periodic Orbits in a two Degree of Freedom Hamiltonian System. Physica 14D, pp. 177-192.

12. Veerman P., Holmes P. 1986. Resonanse Bands in a Two Degree of Freedom Hamiltonian System. Physica 20D, pp. 413-422.

13. Percival I., Richards D. 1982. Introduction to Dynamics. Cambridge Univ. Press, Cambridge.

14. Greenspan B.D., Holmes P. 1983. Homoclinic Orbits, Subharmonics and Global Bifurcations in Forced Oscillations. In "Nonlinear Dynamics and Turbulence", Pitman Advanced Publiching Program.

15. Rosenberg R.M. 1966. Steady State Forced Vibrations. Int. J. Non Linear Mech. 1, pp. 95-108.

16. Kinney W. 1965. On the Geometrization of the Forced Oscillations of Nonlinear Systems having Many Degrees of Freedom. Ph.D. Thesis, Univ. California, Berkeley.

17. Szemplinska-Stupnicka W. 1980. The Resonant Vibration of Homogeneous Non-Linear Systems. Int. J. Non-Linear Mech. 15, pp. 407-415.

18. Hsu C.S. 1960. On the appliation of Elliptic Functions in Nonlinear Forced Oscillations. Quar. App. Math. 17(4), pp. 393-407.

19. Byrd. P., Friedman D. 1954. Handbook of Elliptic Integrals for Engineers and Physicists. Springer Verlag.

20. Kinney W.M., Rosenberg R. 1966. On Steady State Harmonic Vibrations of Nonlinear Systems with Many Degrees of Freedom. J. Appl. Mech. 33(2), pp. 406-412.

21. Hsu C.S. 1965. On the Stability of Periodic Solutions of Nonlinear Dynamical Systems under Forcing. Proceedings CNRS "International Symposioum on Forced Vibration of Nonlinear Systems", 7-12 Sept. 1964, Marseille, France.

22. Rand R. 1971. A Higher Order Approximation for Non-Linear Normal Modes in Two Degree - of - Freedom Systems. Int. J. Non-Linear Mech. 6, pp. 545-547.

23. Rosenberg R., Kuo J. 1964. Nonsimilar Normal Mode Vibrations of Nonlinear Systems Having Two Degrees of Freedom. J. Appl. Mech. 31 (2) , pp. 283-290.

24. Rand R. 1971. Nonlinear Normal Modes in Two-Degree-of-Freedom Systems. J. Appl. Mech. 38(2), pp. 561.

25. Vito P. 1972. An Approximate Method of Treating the Nonlinear Vibrations of Certain Two-Degree-of-Freedom systems. J. Appl. Mech. 39 (2), pp. 620-621.

APPENDIX A: FOURIER EXPANSIONS OF ELLIPTIC FUNCTIONS

The elliptic cosine is expressed in Fourier series, as follows [19]:

$$cn(qt/k) = \sum_{n=0}^{\infty} a_{2n+1} \cos \frac{(2n+1)\pi qt}{2K(k)}$$
$$a_{2n+1} = \frac{2\pi}{kK(k)} \frac{Q^{n+1/2}}{1+Q^{2n+1}} \qquad \text{(A-1)}$$

where $K(\cdot)$ is the complete elliptic integral of the fisrt kind and Q is the elliptic nome, given by $Q = \exp(-\pi K'(k)/K(k))$, $K'(k) = K(1-k)$.

The square of the elliptic cosine is expanded as:

$$cn^2(qt/k) = 1 - \sum_{n=0}^{\infty} b_{2n+1} \sin \frac{(2n+1)\pi qt}{2K(k)}$$
$$b_{2n+1} = \left[\frac{1+k^2}{2k^3} - \frac{(2n+1)^2}{2k^3} \frac{\pi^2}{4K^2(k)} \right] \frac{2\pi}{K(k)} \frac{Q^{n+1/2}}{1-Q^{2n+1}} \qquad \text{(A-2)}$$

and its cube as:

$$cn^3(qt/k) = \sum_{n=0}^{\infty} d_{2n+1} \cos \frac{(2n+1)\pi qt}{2K(k)}$$
$$d_{2n+1} = \frac{1}{2k^2} \left[2k^2 - 1 + (2n+1)^2 \left(\frac{\pi}{2K(k)} \right)^2 \right] \frac{2\pi}{kK(k)} \frac{Q^{n+1/2}}{1+Q^{2n+1}} \qquad \text{(A-3)}$$

Finally, the complete elliptic Integral $K(k)$ is expanded in terms of its modulus as

$$\frac{2K(k)}{\pi} = 1 + \frac{k^2}{2} + O(k^4)$$

APPENDIX B: STABILITY ANALYSIS OF FORCED RESPONCE (SECTION 4.1)

The forced equations of motion are given by:

$$\begin{aligned} \ddot{x}+f_{11}x+f_{13}x^3+f_{23}(x-y)^3 &= f(t) \\ \ddot{y}+f_{11}y+f_{13}y^3+f_{23}(y-x)^3 &= 0 \end{aligned} \qquad \text{(A-5)}$$

Introduce now small variations from the exact steady state motions:

$$\begin{aligned} x(t) &= x^*(t)+\xi(t) \\ y(t) &= y^*(t)+\eta(t) \end{aligned} \qquad \text{(A-6)}$$

Substituting (A-6) into (A-5) and retaining only terms of first order in ξ and η, we obtain:

$$\begin{aligned} \ddot{\xi}+\left[f_{11}+3f_{13}x^{*2}+3f_{23}(x^*-y^*)^2\right]\xi-3f_{23}(x^*-y^*)^2\eta &= 0 \\ \ddot{\eta}+\left[f_{11}+3f_{13}y^{*2}+3f_{23}(y^*-x^*)^2\right]\eta-3f_{23}(y^*-x^*)^2\xi &= 0 \end{aligned} \qquad \text{(A-7)}$$

Taking now into account that at the exact steady state we have,

$$y^*(t)=c\,x^*(t) \qquad \text{(A-8)}$$

equation (A-7) become:

$$\begin{aligned} \ddot{\xi}+\left[f_{11}+3f_{13}x^{*2}+3f_{23}(1-c)^2x^{*2}\right]\xi-3f_{23}(1-c)^2x^{*2}\eta &= 0 \\ \ddot{\eta}+\left[f_{11}+3f_{13}c^2x^{*2}+3f_{23}(c-1)^2x^{*2}\right]\eta-3f_{23}(c-1)^2x^{*2}\xi &= 0 \end{aligned} \qquad \text{(A-9)}$$

This is a set of coupled Hill's equation, which have normal solutions [16] and since the equations are linear, all solutions of (A-9), may be expressed as linear combinations of the normal ones. Thus the question of stability of $\xi(t)$ and $\eta(t)$ may be reduced to the determination of the stability of the normal solutions of (A-9) . These solutions are found by requiring

$$\eta(t)=K\xi(t) \qquad \text{(A-10)}$$

and substituting this relation into (A-10) we get the following set of differential equations in $\xi(t)$:

$$\ddot{\xi}+\left[f_{11}+3f_{13}x^{*2}(t)+3f_{23}(1-c)^2x^{*2}(t)\right]\xi-3f_{23}(1-c)^2x^{*2}(t)K\xi=0$$

$$\ddot{\xi}+\left[f_{11}+3f_{13}c^2x^{*2}(t)+3f_{23}(c-1)^2x^{*2}(t)\right]\xi-\frac{3f_{23}(c-1)^2x^{*2}(t)}{K}\xi=0 \qquad \text{(A-11)}$$

In order for both equations to give the same solution for $\xi(t)$, it is required that the coefficients of $\xi(t)$ in both equations, be equal. That leads to the following values for K :

$$K_{1,2}=\frac{f_{13}(1-c^2)}{2f_{23}(1-c)^2}\pm\left\{1+\left[\frac{f_{13}(1-c^2)}{2f_{23}(1-c)^2}\right]\right\}^{1/2} \qquad \text{(A-12)}$$

and these roots are always real quantities. Then the normal solutions can be computed from any of equation (A-11), with $K=K_i$, $i=1,2$:

$$\ddot{\xi}_i+\left[f_{11}+\left(3f_{13}+3f_{23}(1-c)^2-3f_{23}(1-c)^2K_i\right)x^{*2}(t)\right]\xi_i=0 \qquad i=1,2 \qquad \text{(A-13)}$$

and the solutions of the variational equations (A-9), will be given by [16]:

$$\xi(t)=\xi_1(t)+\xi_2(t)$$
$$\eta(t)=K_1\xi_1(t)+K_2\xi_2(t) \qquad \text{(A-14)}$$

Examine now the variational equation (A-13). The exact steady state solutions is given by equations (4.16) - Section 4.1. Assuming that $\mu_3>0$, for small amplitudes we can express the steady state solution as

$$x^*(t)=X\cos\omega t+O(k^2) \qquad \text{(A-15)}$$

where k^2 is the square of the elliptic modulus and is assumed to be of perturbation order. Substituting ((A-15) into (A-13) and changing the independent variable, we get:

$$\xi_i''+(\delta_i+2\zeta_i\cos 2\tau)\xi_i=0 \quad , \quad i=1,2 \qquad \text{(A-16)}$$

where $(\,)'' \equiv d^2/d\tau^2$, $\omega t = \tau$

and $$\delta_i = \frac{f_{11}}{\omega^2} + \frac{\Lambda_i X^2}{2\omega^2} \quad , \quad \xi_i = \frac{\Lambda_i X^2}{4\omega^2}$$

$$\Lambda_i = 3f_{13} + 3f_{23}(1-c)^2 - 3f_{23}(1-c)^2 K_i$$

and K_i is given by expression (A-12). Equations (A-16) are of Mathiew-type and their stability analysis is well-known. Note that in order that the variational equations (A-9) be stable, both Mathiew equations (A-16) (for $i=1,2$) must be stable.

For each value of X and c , we analyse the stability of equations (A-16) and consequently characterise the respective branches of solutions of figures 24 and 25, as stable or unstable.